Chapter 11
Planetary Gear Drive

With the development of automatic transmission technology, noise reduction and efficiency improvement have become important issues in the field of automotive technology. In AT, the planetary gear train, which can obtain a large gear ratio and meet the requirements of miniaturization and lightweight, has been widely applied, which puts forward higher requirements for the noise and efficiency of the planetary gear train. This chapter will introduce the theoretical calculation and tests of the transmission efficiency and vibration noise of the planetary gear train. The planetary gear train consists of an input shaft, an output shaft and a fixed shaft, all of which are aligned on the same axis. Figure 11.1 shows the power transmission route of the compound planetary gear train in an AT.

Three gear ratios can be obtained by controlling the engagement and disengagement of the clutch and brake in the double-row planetary gear train in Fig. 11.1:

(1) Fig. 11.1a shows the gear ratio 1:0.33 of gear 1.
(2) Fig. 11.1b shows the gear ratio 1:0.617 of gear 2.
(3) Fig. 11.1c shows the overdrive, with the gear ratio of 1:1.44.

See Table 11.1 for the main parameters of gears in the planetary gear train shown in Fig. 11.1.

The gears are made of SCr420H subject to carburizing and quenching heat treatment, with the surface hardness of about 58HRC.

It can be seen from the design parameters of the planetary gear in the AT that the planetary gear and center gear with high tooth and standard tooth are used respectively to change the contact ratio. In order to obtain different accuracy and surface roughness values of tooth surface, two sets of planetary gears and center gears are processed by two different processes (shaving and grinding), in which, one set is only subject to gear shaving, carburizing and quenching and the other set is processed with the same processing technology as the previous set before gear grinding. The former has the accuracy of JIS 3–4 and the tooth surface roughness of about R_aR_{max} 6 μm (R_a

Y. Chen, *Automotive Transmissions*, Springer Tracts in Mechanical Engineering,
https://doi.org/10.1007/978-981-15-6703-2_11

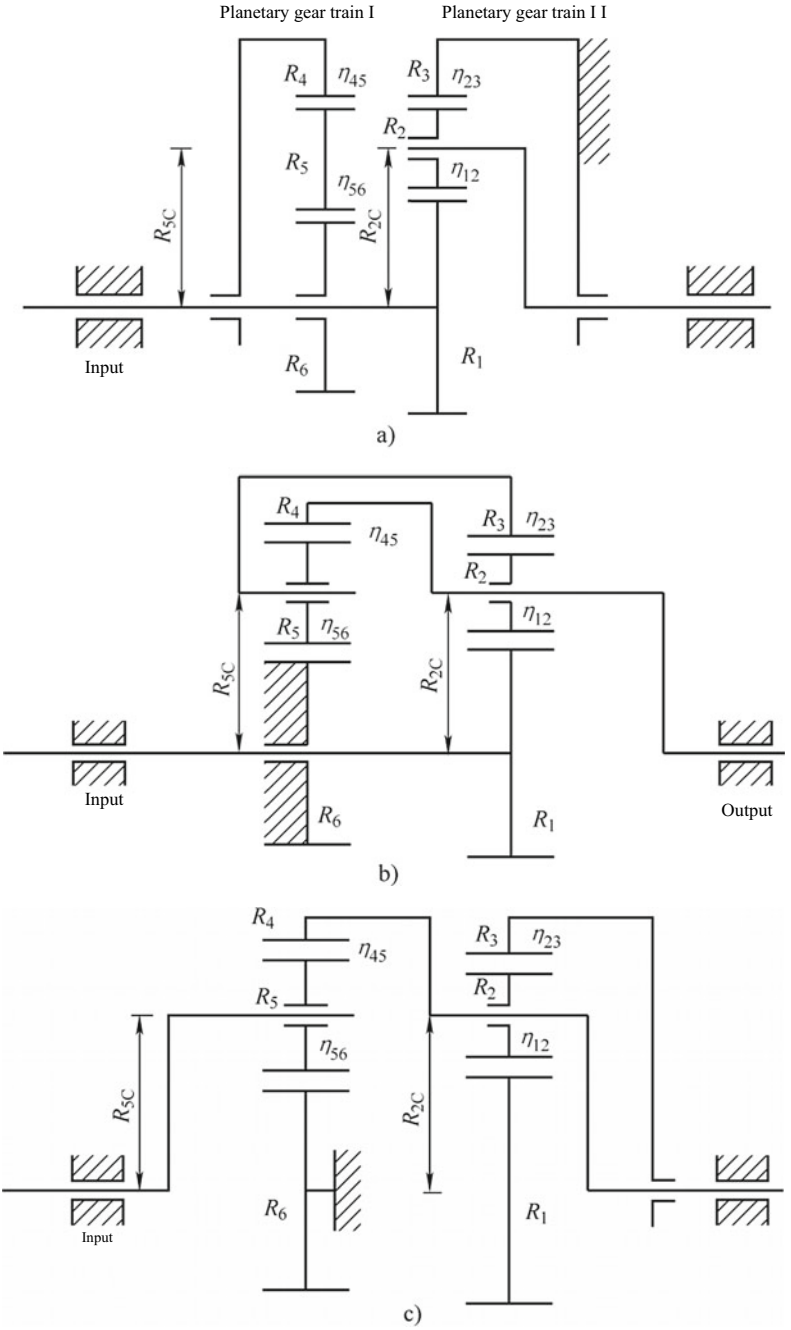

Fig. 11.1 Power transmission route of compound planetary gear train

Table 11.1 Main parameters of gears in planetary gear train

	Planetary gear train I			Planetary gear train II		
Gear type	Planetary gear	Internal gear	Center gear	Planet gear	Internal gear	Center gear
Number of gears	33	21	75	37	19	75
Normal module/mm	1.23			1.23		
Normal pressure angle	20°			20°		
Helical angle	23.3°			23.3°		
Pitch radius/mm	22.09	14.06	50.2	24.76	12.72	50.2
Effective face width/mm	17.0			17.0		
Profile contact ratio A	1.65	–	1.84	1.65	–	1.81
Profile contact ratio B	1.31	–	1.69	1.30	–	1.66
Longitudinal contact ratio	1.74	–	1.74	1.99	–	1.99

1.5 μm). The latter has the accuracy of JIS 0–1 and the tooth surface roughness of about $R_a R_{max}$ 2 μm (R_a 0.5 μm).

11.1 Theoretical Calculation of Transmission Efficiency of Planetary Gear Train

The power transmission efficiency of the planetary gear train depends on the gear mesh efficiency (also known as the benchmark efficiency) when the planetary carrier is fixed. The higher the benchmark efficiency, the higher the efficiency of the planetary gear train. When meshing, the tooth surfaces in contact with each other will slip relative to other contact points other than the meshing point, so there is also tangential friction on tooth surface in addition to the normal force on tooth surface. The magnitude of tangential friction varies with the position of the meshing point on the meshing line. The existence of tangential friction on the tooth surface will reduce the power transmission efficiency and also affect the wear, vibration, noise and meshing effect of the gear teeth.

The benchmark efficiency η_{12} of the external meshed helical gear pair (center gear/planetary gear in the planetary gear train) is

$$\eta_{12} = 1 - \mu\pi\left(\frac{1}{z_A} + \frac{1}{z_B}\right)\left(\varepsilon_1^2 + \varepsilon_2^2 + 1 - \varepsilon_1 - \varepsilon_2\right)/\cos\beta \tag{11.1}$$

where,

μ—average friction factor of tooth surface;
z_A—number of teeth of center gear;
z_B—number of teeth of planetary gear;
ε_1—engaging-in contact ratio;
ε_2—engaging-out contact ratio;
β—helical angle.

The benchmark efficiency η_{23} of the internal meshed helical gear pair (planetary gear/gear ring in planetary gear train) is

$$\eta_{23} = 1 - \mu\pi\left(\frac{1}{z_B} - \frac{1}{z_C}\right)(\varepsilon_1^2 + \varepsilon_2^2 + 1 - \varepsilon_1 - \varepsilon_2)/\cos\beta \tag{11.2}$$

where,

z_C—number of teeth of gear ring.

Suppose the average friction factor $\mu = 0.08$, calculate the benchmark efficiency of two planetary gear sets in the planetary gear train for test using the formulas (11.1) and (11.2), substitute the data in Tables 11.2 and 11.3 and calculate to obtain:

(1) Benchmark efficiency of planetary gear/center gear pair in the first planetary gear set: $\eta_{56} = 0.984806$, benchmark efficiency of gear ring/planetary gear pair: $\eta_{45} = 0.992021$. The benchmark efficiency of the first planetary gear set is calculated as $\eta_{01} = \eta_{45}\eta_{56} = 0.976948$.
(2) Benchmark efficiency of planetary gear/center gear pair in the second planetary gear set: $\eta_{12} = 0.984245$, benchmark efficiency of gear ring/planetary gear pair: $\eta_{23} = 0.991144$. The benchmark efficiency of the second planetary gear set is calculated as $\eta_{02} = \eta_{12}\eta_{23} = 0.975527$.

Table 11.2 Gear parameters of first planetary gear set

Normal pressure angle	$\alpha = 20°$
Normal module	$m_n = 1.23$
Reference helical angle	$\beta = 23.262°$
Tooth addendum	$h_a = 1.17m_n$
Tooth dedendum	$h_f = 1.47m_n$
Number of teeth of sun gear	$z_A = 33$
Number of teeth of planetary gear	$z_B = 21$
Number of teeth of gear ring	$z_C = 75$
Normal modification coefficient of sun gear	$x_{n1} = -0.1539$
Normal modification coefficient of planetary gear	$x_{n2} = 0.1550$
Normal modification coefficient of gear ring	$x_{n2} = 0.1560$

Table 11.3 Gear parameters of second planetary gear set

Normal pressure angle	$\alpha = 20°$
Normal module	$m_n = 1.23$
Reference helical angle	$\beta = 23.2624°$
Tooth addendum	$h_a = 1.17m_n$
Tooth dedendum	$h_f = 1.47m_n$
Number of teeth of sun gear	$z_A = 37$
Number of teeth of planetary gear	$z_B = 19$
Number of teeth of gear ring	$z_C = 75$
Normal modification coefficient of sun gear	$x_{n1} = -0.2652$
Normal modification coefficient of planetary gear	$x_{n2} = 0.2160$
Normal modification coefficient of gear ring	$x_{n2} = 0.1560$

I. Calculation of gear efficiency in gear 1

In Fig. 11.1a, the gear ratio in gear 1 is

$$i_0 = \frac{z'_A}{z'_A + z'_C} \tag{11.3}$$

It is calculated that $i_0 = 0.3304$.

In Fig. 11.1a, the planetary gear R_2 is a drive gear and the center gear R_1 is a driven gear.

Taking into account the benchmark efficiency in Fig. 11.2, the friction power loss ΔL_1 between the center gear R_1 and planetary gear R_2 and the friction power loss ΔL_3 between the planetary gear R_2 and gear ring R_3 are calculated by means of the circumferential force.

When calculating the power loss, the power loss will not occur because the revolution motion will not cause the sliding between the tooth surfaces. On the center gear R_1, the input torque is T_i and the angular velocity is ω_1. The power transmission efficiency without the center gear revolution is

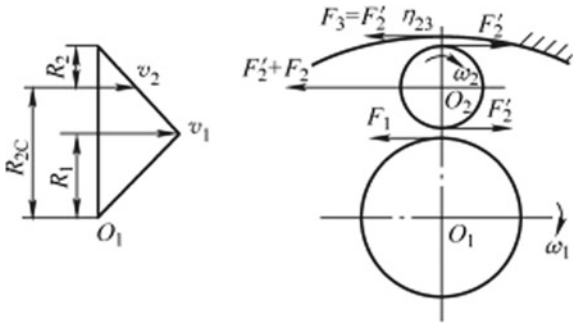

Fig. 11.2 Calculation of gear power loss in gear 1

$$\eta = 1 - \frac{\Delta L_1 + \Delta L_3}{T_i \omega_1} \tag{11.4}$$

where, ΔL_1 and ΔL_3 are calculated according to the angular velocity of each gear relative to the planetary carrier at the meshing point, namely

$$\Delta L_1 = F_1 R_1 \omega_1' (1 - \eta_{12}) \tag{11.5}$$

$$\Delta L_3 = F_2' R_2' \omega_2' (1 - \eta_{23}) \tag{11.6}$$

where,

ω'_1 and ω'_2—angular velocity of center gear and planetary gear relative to the planetary carrier.

The following relations

$$F_2' = \eta_{12} F_1; \omega_2' = \frac{\omega_1' R_1}{R_2}; \omega_1 = \frac{\omega_1' (R_2 + R_3)}{R_3}$$

are substituted into the power transmission efficiency formula to obtain $\eta = 0.98361$.

II. **Theoretical efficiency calculation of planetary gear in gear 4**

The circumferential force on the gears in gear 4 is shown in Fig. 11.3.

In the figure, ω_{5C} is the angular velocity of planetary carrier. The relative angular velocities ω'_1 and ω'_5 are determined and the friction power loss ΔL_1 between the center gear and planetary gear and the friction power loss ΔL_3 between the planetary gear and gear ring are calculated by

$$\Delta L_1 = F_5 (1 - \eta_{56}) R_6 \omega_1' \tag{11.7}$$

$$\Delta L_3 = F_5' (1 - \eta_{45}) R_4 \omega_5' \tag{11.8}$$

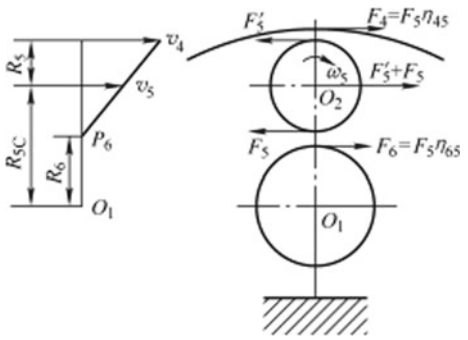

Fig. 11.3 Circumferential force acting on the gears in gear 4

where

$$\omega_1' = \omega_{5C};\ \omega_5' = \omega_4 - \omega_{5C}$$

The above and the following relations

$$\omega_4' = \frac{2R_{5C}}{R_4}\omega_{5C};\ F_5 = F_5';\ R_6 + 2R_5 = R_4$$

are substituted into the efficiency formula $\eta = 1 - (\Delta L_1 + \Delta L_1)/(T_5\omega_5)$ to obtain $\eta = 0.992921$.

III. **Derivation of theoretical efficiency formulas of gears in gear 2**

1. **Derivation of approximate formulas for theoretical efficiency not using mechanism coincidence**

The circumferential force acting on the gears in gear 2 is shown in Fig. 11.4. The relationship between the circumferential forces of each gear is

$$\begin{cases} F_{22} = F_{21} = F_{2C}/2 = F_1 = F_3 \\ F_4 = F_{52} = F_5 = F_6 = F_{5C}/2 \\ F_{5C}R_{5C} = F_3R_3 = F_1R_3 \\ F_4R_4 = F_{2C}R_{2C} \end{cases} \tag{11.9}$$

The circulation power is

$$L_C = R_{2C}\frac{R_3R_4}{2R_{2C}R_{5C}}F_1\omega_{2C} = \omega_3R_3F_3 \tag{11.10}$$

According to Fig. 11.2b, there is the following angular velocity relation

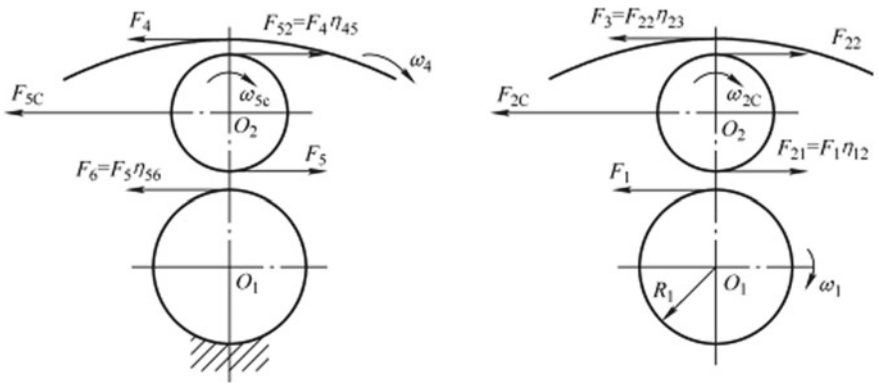

Fig. 11.4 Circumferential force acting on the gears in gear 2

$$\omega_6 = 0;\ \omega_{5C} = \omega_3;\ \omega_4 = \omega_{2C};\ \omega_4 R_4 = 2\omega_{5C} R_{5C}$$

Taking into account the benchmark efficiency of the mechanism in Fig. 11.4, the power loss ΔL_{12} between the center gear R_1 and planetary gear R_2 in the second planetary gear set and the power loss ΔL_{23} between the planetary gear R_2 and gear ring R_3; the power loss ΔL_{45} between the gear ring R_4 and planetary gear R_5 in the first planetary gear set, and the power loss (friction heat loss) ΔL_{56} between the planetary gear R_5 and fixed center gear R_6 are calculated by means of the circumferential force. The revolution motion of the planetary gear is independent of the slip between the tooth surfaces. Here, the revolution rate C is introduced, so the proportion of the rotation component of the input angular velocity is $1 - C$.

The calculation process of the revolution rate is as follows: the angular velocity ω_{2C} of planetary carrier (R_{2C}) and the angular velocity ω_3 of gear ring R_3 are positive. If $\omega_{2C} < \omega_3$, the revolution rate is

$$C_3 = (2\omega_3 - \omega_{2C})/\omega_3 \tag{11.11}$$

If $\omega_{2C} < \omega_1$, the revolution rate is

$$C_1 = \omega_{2C}/\omega_1 \tag{11.12}$$

If $\omega_{5C} < \omega_4$, the revolution rate is

$$C_4 = \omega_{5C}/\omega_4 \tag{11.13}$$

The approximate formula for the efficiency of the dual-planetary gear set in Fig. 11.2b is

$$\eta = 1 - \frac{\Delta L_{12} + \Delta L_{23} + \Delta L_{45} + \Delta L_{56}}{F_{2C} R_{2C} \omega_{2C} - F_{22} R_3 \omega_3} \tag{11.14}$$

where

$$\begin{cases} \Delta L_{12} = F_1(1 - \eta_{12})(1 - C_1)\omega_1 R_1 \\ \Delta L_{23} = F_{22}(1 - \eta_{23})(1 - C_3)\omega_3 R_3 \\ \Delta L_{45} = F_4(1 - \eta_{45})(1 - C_4)\omega_4 R_4 \\ \Delta L_{56} = F_6(1 - \eta_{56})C_4\omega_4 R_6 \end{cases} \tag{11.15}$$

Finally, it is obtained that $\eta = 0.977355$.

2. **Derivation of approximate formulas for theoretical efficiency using mechanism coincidence**

In the dual-planetary gear set shown in Fig. 11.2b, the power will be shunted only when the center gear of the planetary gear set is fixed. A part of power flows back

to R_{2C} from the gear ring R_4 and generates power cycle between the first and second planetary gear sets. The power passing through the planetary carrier R_{2C} is greater than the input/output power. The gear ring R_3 and center gear R_1 are the drive part and R_{2C} is the driven part. The second planetary gear set makes up a differential mechanism.

In the following calculation process, the dual-planetary gear set is divided into two to calculate its efficiency.

(1) Component 1: as shown in Fig. 11.5, the sun gear R_1 is fixed, the theoretical circulation power is input from R_3 and output from R_{2C}. In this process, the efficiency is η_{2C3}
The circulation power is

$$L_C = L_{C3} = F_3 R_3 \omega_3 = \omega_3 R_3 F_3 \tag{11.16}$$

Output power

$$L_{C3} = L_{C3}\eta_{2C3} \tag{11.17}$$

(2) Component 2: as shown in Fig. 11.6, the gear ring R_3 is fixed and the input drive power of the center gear R_1 is

$$L_1 = F_1 R_1 \omega_1 \tag{11.18}$$

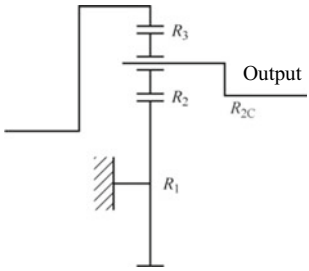

Fig. 11.5 Analysis of component 1

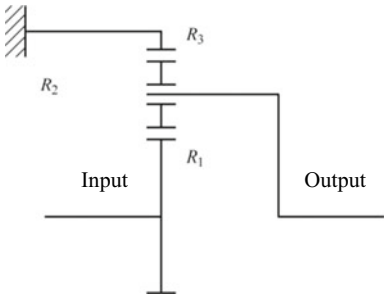

Fig. 11.6 Analysis of component 2

The power is output from the planetary carrier R_{2C} and the efficiency in the process is η_{2C1}. Then the output power is

$$L_{C1} = F_1 \omega_1 R_1 \eta_{2C1} \tag{11.19}$$

(3) Theoretical transmission efficiency (Figs. 11.7, 11.8 and 11.9)

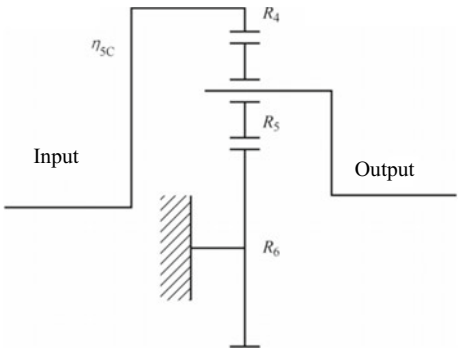

Fig. 11.7 R_6 fixed

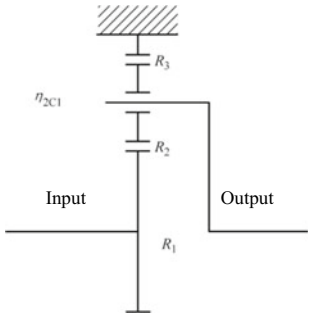

Fig. 11.8 R_3 fixed

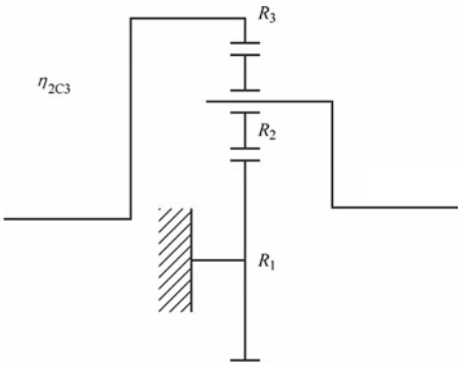

Fig. 11.9 R_1 fixed

$$\eta = \frac{L_{C1} + L_{C3} - L_{C3}/\eta_{5C}}{F_1 R_1 \omega_1} \tag{11.20}$$

where,
η_{5C}—efficiency when the center gear R_6 in the first planetary gear set is fixed, driven by the gear ring R_4 and output by the planetary carrier R_{5C}.

Then

$$\begin{cases} L_{C1} = F_1 R_1 \omega_1 \eta_{2C1} \\ L_{C3} = F_3 R_3 \omega_3 \eta_{2C3} \\ L_{C3} = L_C = F_3 R_3 \omega_3 \end{cases} \tag{11.21}$$

$$F_{3th} = F_{1th} \tag{11.22}$$

$$\omega_3 = \frac{R_4 \omega_{2C}}{2R_{5C}} = \frac{R_1 R_4 \omega_1}{2R_2 C_2 R_{5C} - R_3 R_4} \tag{11.23}$$

$$\eta_{5C} = \frac{\eta_{O1} + i_O}{1 + i_O} \tag{11.24}$$

$$i_O = R_4/R_6 \tag{11.25}$$

Figure 11.9 R_1 fixed It is calculated that $\eta_{5C} = 0.99296$.

$$\eta_{2C1} = \frac{1 + \eta_{O2} i_O}{1 + i_O} \tag{11.26}$$

$$i_O = R_3/R_1 \tag{11.27}$$

It is calculated that $\eta_{2C1} = 0.98361$.

$$\eta_{2C3} = \frac{\eta_{O2} z'_A + z'_C}{z'_A + z'_C} \tag{11.28}$$

It is calculated that $\eta_{2C3} = 0.99192$.
Through the above formulas, $\eta = 0.97042$.

IV. **Theoretical efficiency calculation considering bearing loss**

The main reasons that affect the efficiency of planetary gear include tooth surface friction loss, bearing friction loss, lubricant churning loss and air drag loss. To analyze the transmission efficiency of tooth surface of planetary gear, it is necessary to find out the bearing friction loss, lubricant churning loss and air drag loss, among which, the lubricant churning loss and air drag loss can be measured by no-load test. The bearing loss in the transmission is theoretically analyzed below.

(I) **Analysis of bearing friction**

The bearing friction moment can be measured experimentally and there are four types of friction:

(1) Pivoting friction.
(2) Friction caused by minute slip of rotary parts.
(3) Slip contact friction.
(4) Lubricant viscosity.

The friction loss varies with the bearing form, working speed and lubrication conditions.

The bearing friction can be divided into dynamic friction and static friction, and the dynamic friction is related to working load and speed. Items (1), (2) and (3) above, namely, the contact between bearing metal parts are determined by the load; item (4) is determined by the speed.

(II) **Transmission efficiency of thrust bearing**

The needle roller of thrust bearing under axial load will produce corresponding friction force. In the case of good lubrication, the sliding friction factor is about 0.006; in case of poor lubrication, the friction factor is about 0.015.

1. **Transmission efficiency of thrust bearing in gear 1**

Figure 11.10 shows the installation positions of the bearings in the planetary gear train for test. The arrows in Fig. 11.11 indicate the direction of the thrust on the center gear and gear ring of the gears in gear 1 (single planetary gear set).

Through the analysis of the thrust on the planetary gear train in Fig. 11.11, the center gear R_1 and gear ring R_3 in Fig. 11.1a have thrust effect on the thrust bearings 5 and 6 (Fig. 11.10) and the transmission efficiency is

$$\eta_{b1} = 1 - \frac{F_1 \tan\beta R_{h5} \mu_{r1} (\omega_1 - \omega_{2C})}{F_1 R_1 \omega_1} \tag{11.29}$$

$$\eta_{h2} = 1 - \frac{F_1 \tan\beta R_{b5} \mu_{r1} \omega_{2C}}{F_1 R_1 \omega_1} \tag{11.30}$$

where,

μ_{r1}—friction factor of thrust bearing;
R_{b5}—rotation radius of the roller center of bearing 5;
R_{b6}———rotation radius of the roller center of bearing 6.

2. **Transmission efficiency of thrust bearing in gear 2**

Figure 11.12 shows the direction of the thrust of the 2 speed planetary gear train on the center gear and gear ring. The thrust of the planetary gear train in Fig. 11.12 is analyzed. The thrust bearings 5 and 6 are subject to the thrust of the center gear R_1 and gear ring R_3 in Fig. 11.1b and the transmission efficiency is

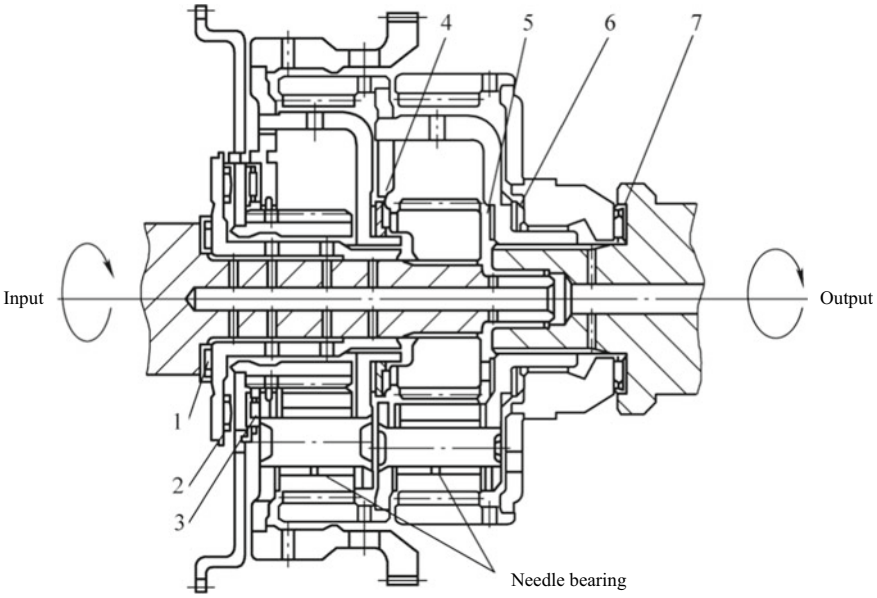

Fig. 11.10 Installation positions of the bearings in the planetary gear train for test. 1–7—bearing

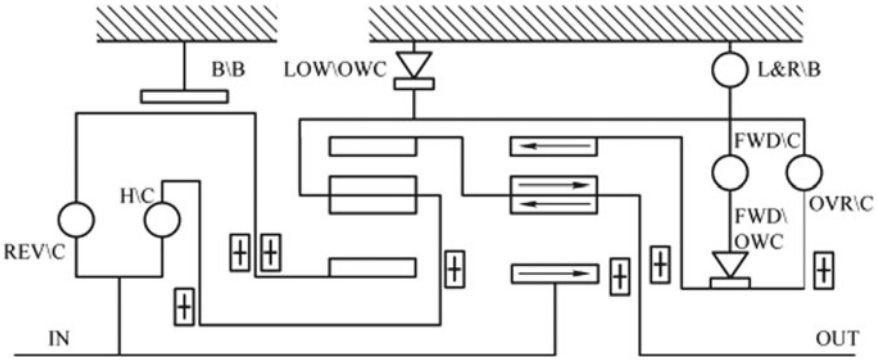

Fig. 11.11 Force on the center gear and gear ring in gear 1

$$\eta_{h3} = 1 - \frac{F_{3th} \tan \beta R_{b5} \mu_{r1} \omega_3}{F_1 R_1 \omega_1} \tag{11.31}$$

The thrust bearing 4 is subject to the thrust of the gear ring R_4 and the transmission efficiency is

$$\eta_{b4} = 1 - \frac{F_4 \tan \beta R_{b4} \mu_{r1} (\omega_1 - \omega_{2C})}{F_1 R_1 \omega_1} \tag{11.32}$$

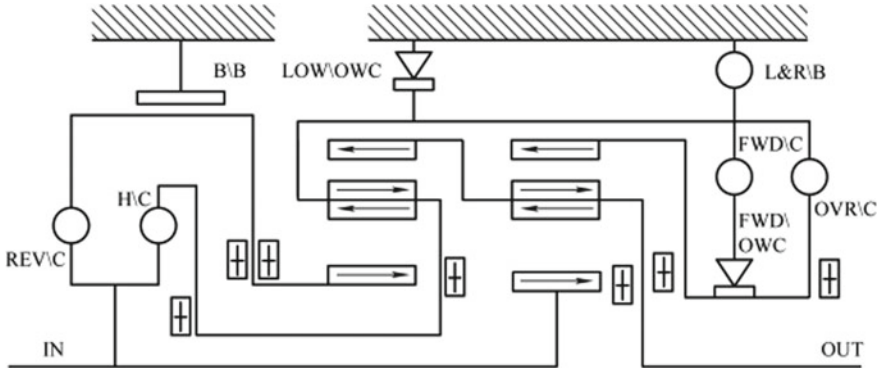

Fig. 11.12 Force on the center gear and gear ring in gear 2

where,

R_{b4}—rotation radius of the roller center of bearing 4.

(III) **Transmission efficiency of needle bearing**

The crowded needle bearing installed on the planetary gear is free of retainer, inner ring and outer ring, maximizing the miniaturization, increasing the effective radius and greatly increasing the rated load of the crowded needle bearing. The planetary gear and crowded needle bearing are shown in Fig. 11.13. Figure 11.14 is the installation diagram of crowded needle bearing.

The crowded needle bearing has no retainer, so the roller will tilt, which will produce axial thrust acting on the inner ring and the outer ring in opposite direction. Because the length of the needle roller is larger than its diameter, the outer ring flange

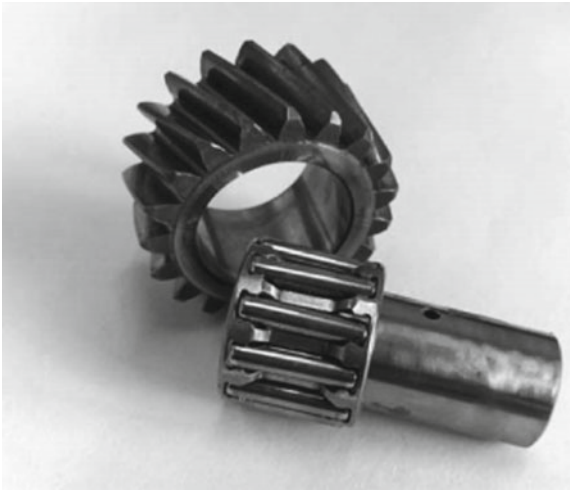

Fig. 11.13 Planetary gear and crowded needle bearing

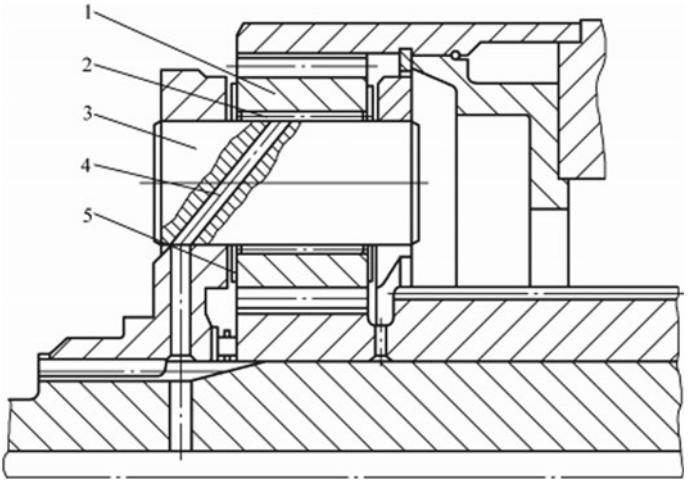

Fig. 11.14 Installation diagram of crowded needle bearing. 1—milled planetary gear (carburizing and quenching), 2—needle roller, 3—carburized and quenched shaft, 4, 5—oil passage

is unable to limit the rolling direction of the needle roller, which may easily cause the tilt of the needle roller and will have a large influence on the friction.

The gears used in the planetary gear train of AT are helical gears, and the axial force generated by the meshing of the gear ring and planetary gear is opposite to that generated by the meshing of the center gear and planetary gear, which will aggravate the tilt trend of roller. The bearing load caused by the tilt of the needle roller accounts for a portion of the bearing axial load. The friction resistance caused by the tilt of the needle roller will increase the friction force.

1. **Transmission efficiency of needle bearing in gear 1**

The approximate formula for the transmission efficiency η_{B6} of the crowded needle bearing used by the planetary gear in the second planetary gear set is

$$\eta_{b6} = 1 - \frac{F_{P1} R_{b1} \mu_{r1}}{F_1 R_1 \omega_1} \frac{R_1 (1 - C_1) \omega_1}{R_2} \tag{11.33}$$

$$F_{P1} = F_1 \sqrt{1 + [(4R_2/B_1) \tan \beta]^2} \tag{11.34}$$

where,

F_{P1}—compound radial load of planetary gear R_2 acting on the needle bearing;
μ_{r1}—friction factor of thrust bearing;
ω_1—angular velocity of input shaft;
C_1—revolution rate, $C_1 = \omega_{2C}/\omega_1$, in which, ω_{2C} is the angular velocity of output shaft.

$$C_1 = \omega_{2c} \div \omega_1. \tag{11.35}$$

F_1—circumferential force acting on the sun gear R_1;
B_1—needle roller length of the needle bearing on the planetary gear R_2;
R_{b1}—bearing bore diameter;
β—helical angle of planetary gear;
R_1—pitch radius of sun gear R_1;
R_2—pitch radius of planetary gear R_2.

2. Transmission efficiency of needle bearing in gear 2

In the 2 speed dual-planetary gear set shown in Figs. 11.1b and 11.15, 10 bearings are subject to the radial and axial loads by the gears and support the components in the planetary gear train, in which, 7 bearings are crowded needle bearings.

When the radial and axial loads act on the crowded needle bearings in the second planetary gear set, the theoretical transmission efficiency is

$$\eta_{b7} = 1 - \frac{F_{P1} R_{b1} \mu_{r1}}{F_1 R_1 \omega_1} \frac{R_1 (1 - C_1) \omega_1}{R_2} \tag{11.36}$$

The theoretical transmission efficiency of the crowded needle bearings in the first planetary gear set is

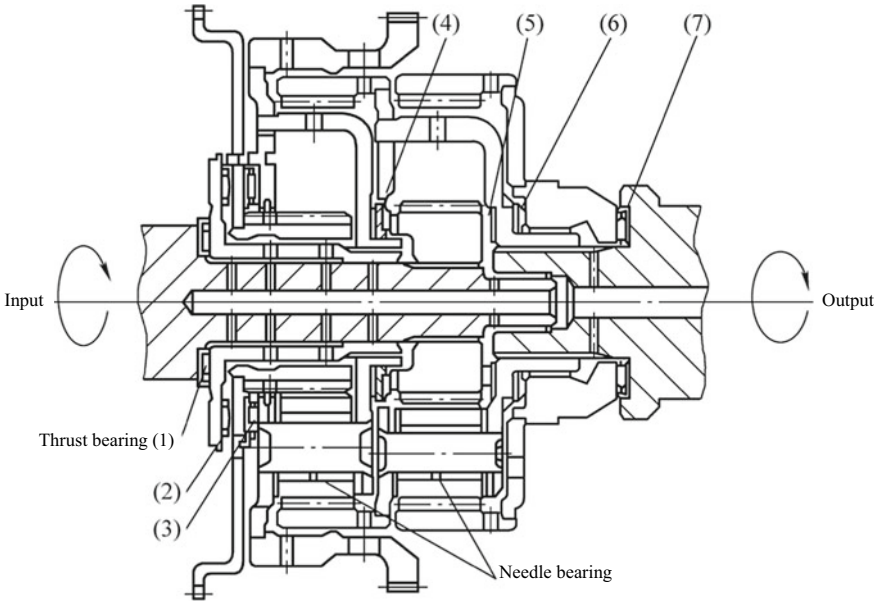

Fig. 11.15 Dual-planetary gear set

$$\eta_{b8} = 1 - \frac{F_{P2} R_{b2} \mu_{r2}}{F_1 R_1 \omega_1} \frac{R_4 (1 - C_4) \omega_4}{R_5} \tag{11.37}$$

$$F_{P2} = F_1 \sqrt{1 + [(4R_2/B_2) \tan \beta]^2} \tag{11.38}$$

where,

F_{P2}—compound radial load of planetary gear R_5 acting on the needle bearing;
μ_{r2}—friction factor of thrust bearing;
C_4—revolution rate, $C_4 = \omega_{5C}/\omega_4$, in which, ω_4 is the angular velocity of gear ring R_4 in the first planetary gear set;
ω_{5C}—angular velocity of revolution of planetary gear R_5 in the first planetary gear set;
B_2—needle roller length of the needle bearing on the planetary gear R_5;
R_{b2}—bearing bore diameter;
R_4—pitch radius of gear ring R_4;
R_5—pitch radius of planetary gear R_5.

V. **Theoretical calculation of overall efficiency**

1. **Overall efficiency of 1 speed gears**

The theoretical overall efficiency η_{rth} of the 1 speed gears (single planetary gear set) is

$$\eta_{rth} = \eta_{th} \eta_{b1} \eta_{b2} \eta_{b6} \eta_0 \tag{11.39}$$

where,

η_{th}—tooth surface benchmark efficiency;
η_{b1}, η_{b2}—transmission efficiency of thrust bearing;
η_{b6}—efficiency of needle bearing;
η_0—idle efficiency of 1 speed single planetary gear set test.

Affected by the lubricant churning loss and the air drag loss from the gear drive, it is difficult to calculate the idle efficiency η_0, which is mainly affected by the speed and is unrelated to the load, so its value can be tested through a blank experiment.

2. **Theoretical overall efficiency of 2 speed gears**

The theoretical overall efficiency of the 2 speed gears (dual-planetary gear set) is

$$\eta_{rth} = \eta_{th} \eta_{b3} \eta_{b4} \eta_{b5} \eta_{b7} \eta_{b8} \eta_0 \tag{11.40}$$

where,

η_{b3}, η_{b4} and η_{b5}—transmission efficiency of thrust bearing;
η_{b7} and η_{b8}—efficiency of needle bearing;
η_0—idle efficiency of 2 speed dual-planetary gear set test.

11.2 Transmission Efficiency Test of Planetary Gear Train

The transmission used in the test is of dual-planetary gear set type, as shown in Fig. 11.15. The transmission has four gears and its power transmission route is shown in Fig. 11.16.

In order to reduce the impact of vibration and elastic deformation, the transmission case is required to be stiff enough; a coupling is arranged on the fixed part or the transmission shaft to ensure that the gears mesh evenly when working. Each part shall have high manufacture and assembly accuracy, and the position error at the center of rotation of the input and output shafts shall be controlled below 0.025 mm.

Three lubricants are used in the test. A is mineral oil commercially available for ordinary lubrication, B is the automobile ATF and C is the steam turbo-compressor lubricant (mineral oil). The ATF is mainly used in this test.

The relationship between the kinematic viscosity and temperature of the three lubricants is shown in Fig. 11.17.

The composition and principle of the power absorption type gear efficiency test bench for the test are shown in Fig. 11.18. The drive motor drives the test planetary gear train to work through the CVT, V-belt, coupling and torque estimator. The load is loaded on the output shaft of the planetary gear train by the drum brake via the output torque estimator and coupling.

Before the test, the bench shall run smoothly for 20 min, and then gradually load from the no-load state for the test. The speed of the input shaft is controlled within the range of 500–3000 r/min, and the torque is controlled within the range of 0–85 N m. In order to make the lubrication mode consistent with AT, the oil pumping shall be used for forced lubrication, and the three injectors near the center gear and one injector in the upper part of the center gear are used to provide lubricant for the planetary gear set. The lubricant temperature at the injectors is determined by a temperature sensor.

In fact, it is difficult to determine the gear transmission efficiency. Although it is considered to calculate the transmission efficiency (overall efficiency) through the theoretical efficiency calculation and test method of the meshing loss, the influence factors and mechanical relations are not easy to study. The structure of the planetary gear train is more complex and it is more difficult to accurately determine its transmission efficiency.

Under the forced lubrication conditions, the power loss types affecting the overall efficiency η of the planetary gear train are as follows:

(1) Meshing tooth surface friction loss ΔL_1.
(2) Bearing friction loss ΔL_2.
(3) Churning loss ΔL_3 caused by the rotating parts such as gear churning the lubricant.
(4) Air drag loss ΔL_4 generated in the rotation of parts such as gear.

In the above items, (1) and (2) are load influence, (3) and (4) are speed influence. The overall efficiency is

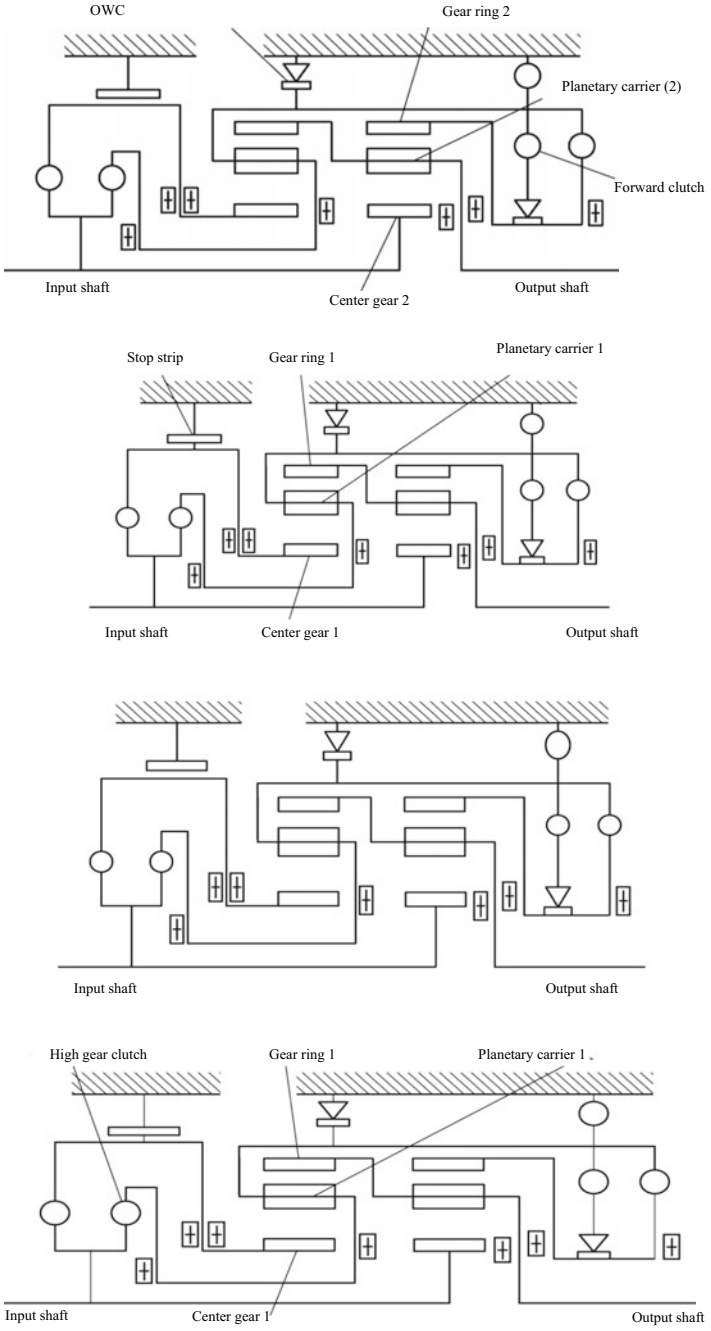

Fig. 11.16 Power transmission route of 4 gears

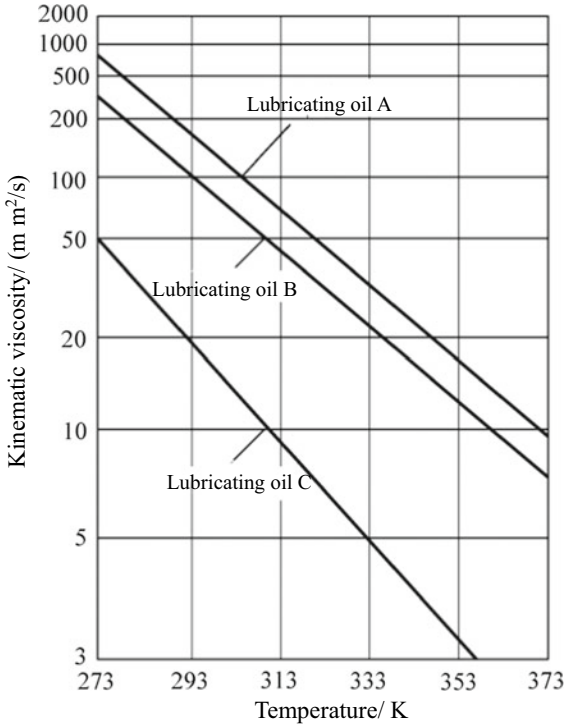

Fig. 11.17 Relationship between the kinematic viscosity and temperature of three lubricants

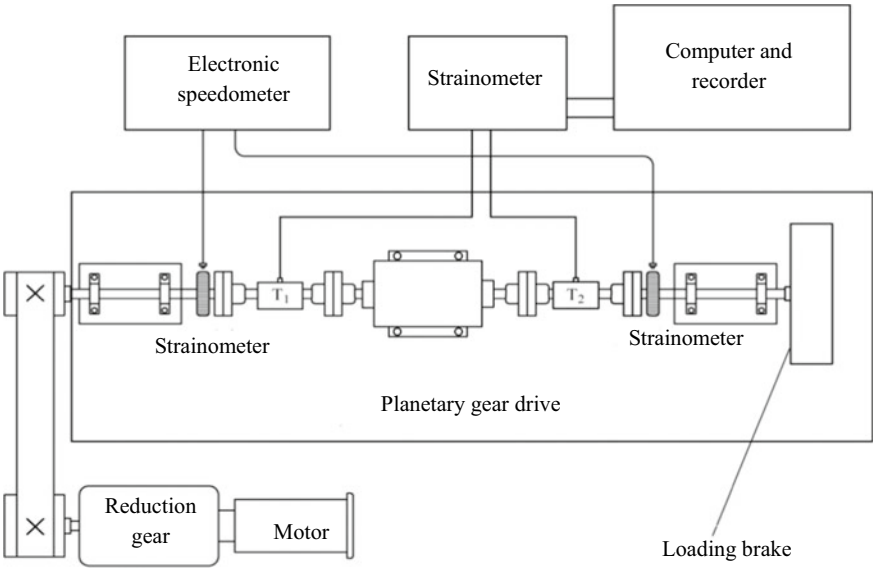

Fig. 11.18 Composition and principle of the power absorption type gear efficiency test bench

$$\eta = 1 - \frac{\Delta L_1 + \Delta L_2 + \Delta L_3 + \Delta L_4}{T_i \omega_1} \tag{11.41}$$

where,

T_i—input torque;
ω_1—drive angular velocity.
$\Delta L_3 + \Delta L_4$ may be measured in no-load state and ΔL_2 may be calculated from the bearing loss formula.

After the power loss $\Delta L_3 + \Delta L_4$ in the idling is measured, the theoretical calculation efficiency mentioned above is compared with the measured efficiency to check the influence of the power cycle and other factors on the overall efficiency.

The single and dual-planetary gear sets are tested respectively, and the influence of the variables controlled and adjusted, including speed, load, gear accuracy, gear contact ratio, lubricant type, temperature and flow, on the transmission efficiency is analyzed finally.

I. **Influence of churning loss on overall efficiency**

At the same temperature, the higher the viscosity of the lubricant, the greater the churning loss, as shown in Fig. 11.19. The lower the temperature of the lubricant, the greater the churning loss, as shown in Fig. 11.20. As can be seen from Fig. 11.21, at the same temperature, the higher the lubricant flow and gear speed, the greater the churning loss.

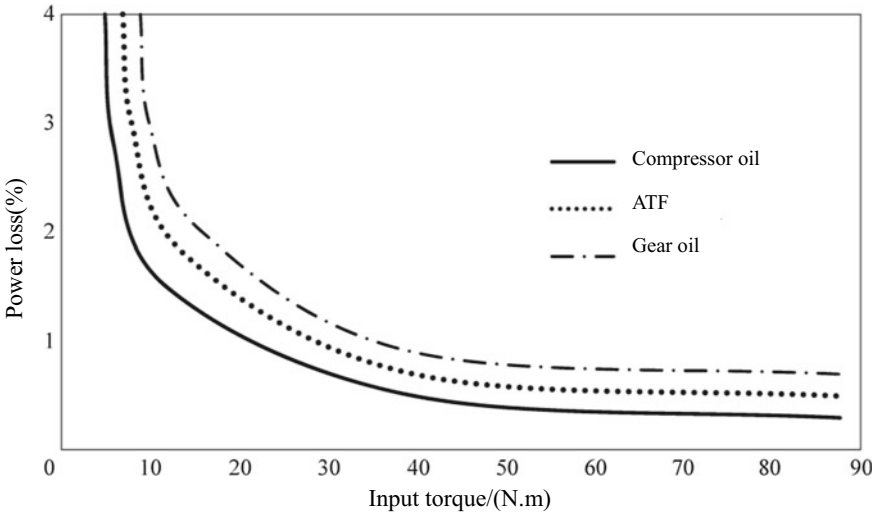

Fig. 11.19 Relationship between lubricant viscosity and churning loss

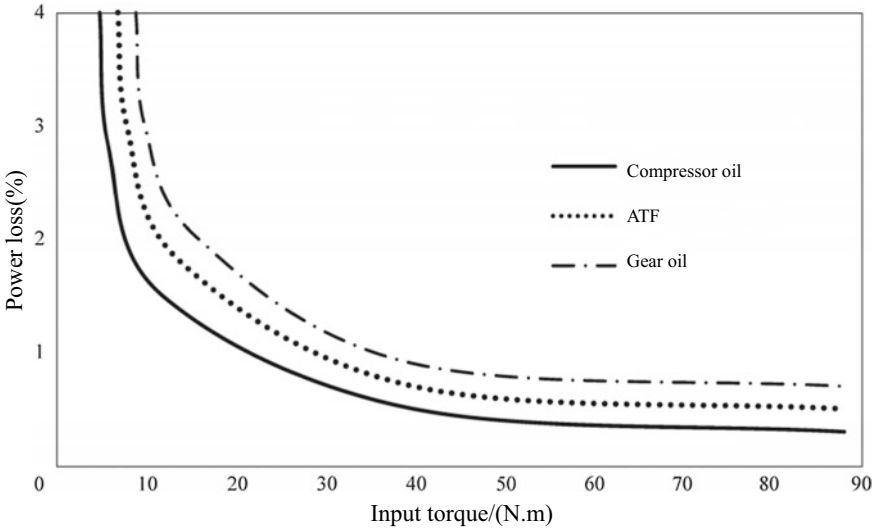

Fig. 11.20 Relationship between lubricant temperature and churning loss

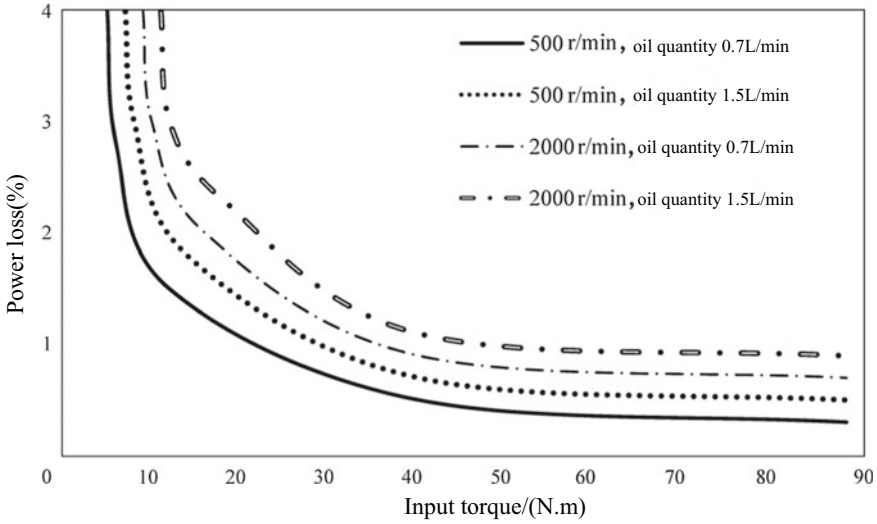

Fig. 11.21 Relationship between lubricant flow and gear speed and churning loss

II. **Influence of processing technology on overall efficiency**

The set of center gear and planetary gear of 1 speed gear for the test is shaved and the other set is ground. The test results are shown in Fig. 11.22 and the transmission efficiency of gears manufactured by the two processing technologies is slightly different. The transmission efficiency of the ground gears is about 0.5% higher than

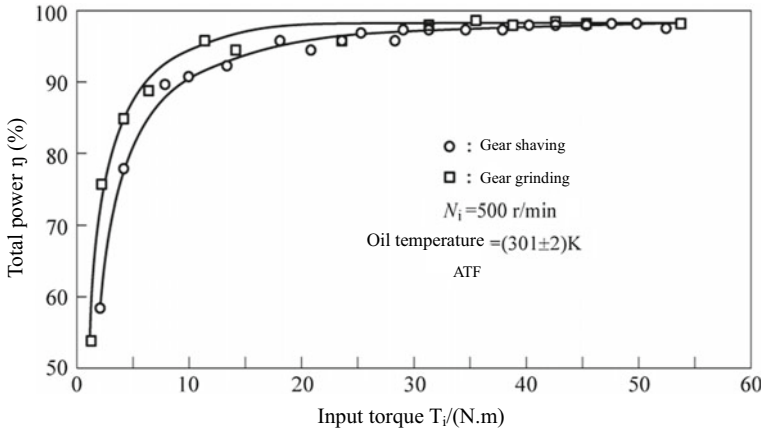

Fig. 11.22 Influence of processing technology on overall efficiency

that of the shaved gears. This is because the tooth surface of the shaved gears is rough and less accurate with large tooth surface friction factor.

III. **Influence of speed on overall efficiency**

The 1 speed gear is selected for the test, with the gear ratio of 1:0.33, the processing technology of gear shaving and the input speed of 500, 1500 and 2000 r/min. The lubricant with high viscosity is selected.

The test results are shown in Fig. 11.23. The corresponding transmission efficiency has little difference at the speed of 500 and 1000 r/min; but it decreases obviously at the speed 2000 r/min. It is speculated that the lubricant churning loss and the air drag loss are related to the square of the speed.

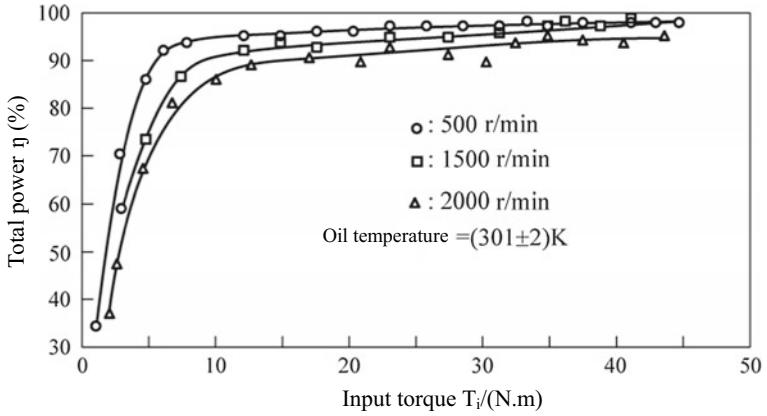

Fig. 11.23 Influence of speed on overall efficiency

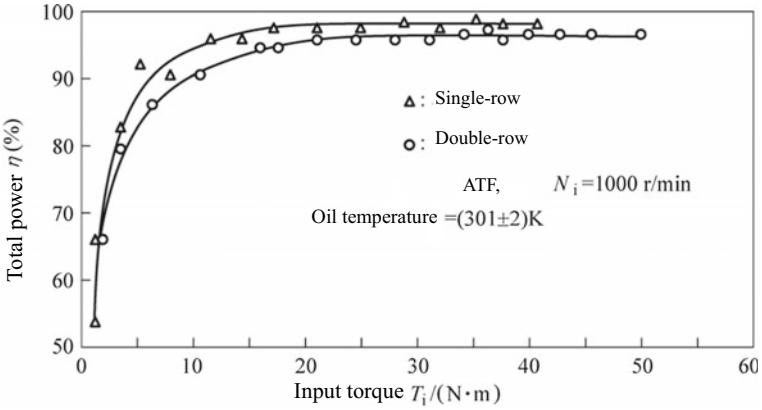

Fig. 11.24 Influence of single and dual-planetary gear sets on overall efficiency

IV. Influence of single and dual-planetary gear sets on overall efficiency

Figure 11.24 shows the comparison of the transmission efficiency test results of single and dual-planetary gear sets. The processing technology is gear grinding. The center gear of the first planetary gear set in the dual-planetary gear set is fixed and the second planetary gear set is of differential form. The 2 speed power cycle transmission route of a power ($F_{22}R_3\omega_3$) is: gear ring $R_3 \rightarrow$ planetary gear $R_2 \rightarrow$ planetary carrier $R_{2C} \rightarrow$ gear ring $R_4 \rightarrow$ planetary carrier $R_{5C} \rightarrow$ gear ring R_3. The efficiency reduction caused by the power cycle is also analyzed in the theoretical calculation of the previous section.

V. Influence of contact ratio on overall efficiency

The test only changes the gear contact ratio of the planetary gear train and the influence of the contact ratio on the overall efficiency is shown in Fig. 11.25. The contact ratio 1.30/1.66 is represented by "□", while the contact ratio 1.65/1.82 is represented by "△". The efficiency decreases in the large contact ratio because the increase in the relative slippage of two meshing teeth results in the friction loss increase.

VI. Influence of lubricant temperature and flow on overall efficiency

The influence of the lubricant temperature on the transmission efficiency is shown in Fig. 11.26. The lubricant temperature is high and the total efficiency is high at low load because of low lubricant viscosity and small churning loss at high temperature.

The influence of the lubricant flow on the transmission efficiency is shown in Fig. 11.27. When the lubricant flow is increased, the overall efficiency will decrease significantly; but after the load is increased, the influence of the lubricant flow on the efficiency will decrease. It is because that the increase in the lubricant flow will make the viscous resistance increase and the churning loss is not affected by the load on the tooth surface.

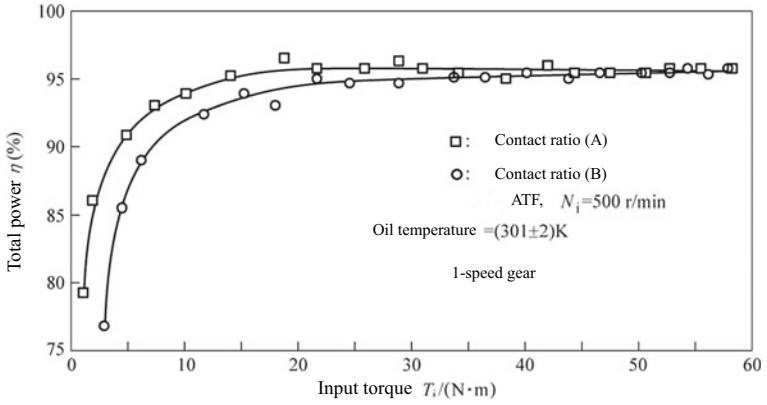

Fig. 11.25 Influence of contact ratio on overall efficiency

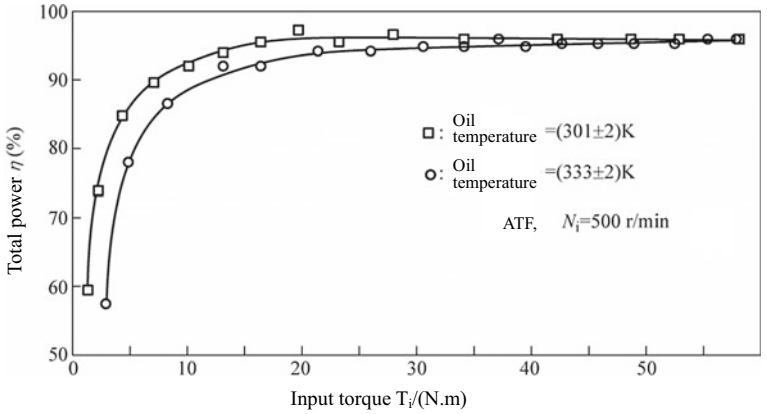

Fig. 11.26 Influence of lubricant temperature on overall efficiency

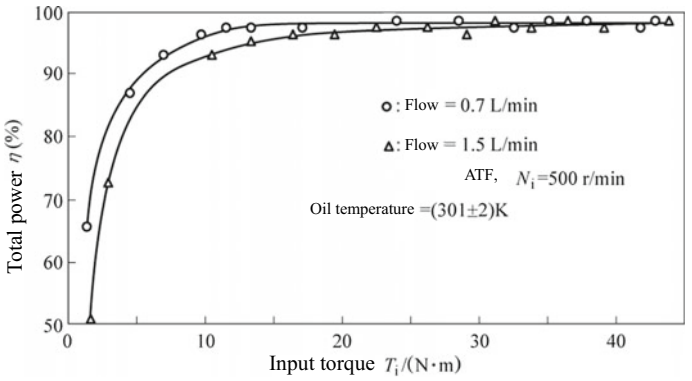

Fig. 11.27 Influence of lubricant flow on overall efficiency

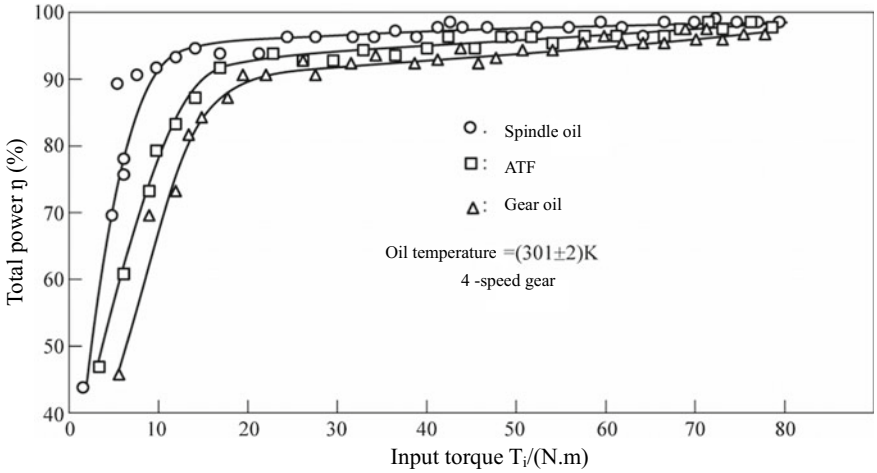

Fig. 11.28 Influence of lubricant type on overall efficiency

VII. **Influence of lubricant type on overall efficiency**

The 4 speed gear is selected for the test, with the gear ratio of 1:1.44, the processing technology of gear grinding and the input speed of 500 r/min. The test results are shown in Fig. 11.28. Among the three lubricants applied, that with low viscosity has high overall efficiency, but the influence of viscosity on transmission efficiency is decreased with the increase of load.

Even though the difference in the kinematic viscosity of the lubricant is up to 6 times, the influence of the lubricant type on the transmission efficiency is not significant when the medium load or above is applied.

VIII. **Theoretical calculation and test results analysis of overall efficiency**

Figure 11.29 shows the theoretical efficiency and test efficiency of the input torque and tooth surface meshing of the 1 speed gear at the input speed 500 r/min, as well as the relationship between the efficiencies with consideration to the churning loss and bearing loss. The input torque is 0–50 N m. The tooth surface benchmark efficiency η_{th} of the gear is calculated with the average friction factor between tooth surfaces $\mu = 0.08$ and marked with straight line in Fig. 11.29; the dash-dotted line represents the efficiency curve including churning loss and air loss; the dotted line represents the efficiency calculated after considering the needle bearing friction factor $\mu_{r1} = 0.0025$ and thrust bearing friction factor $\mu_{r2} = 0.008$ ($\eta_{rth} = \eta_{th}\ \eta_{b1}\ \eta_{b2}\ \eta_{b6}\ \eta_0$).

μ_{r1} is inversed by the test value of η_{rth} to obtain $\mu_{r1} = 0.011$. That is, the measured overall efficiency under this friction factor is at the same level with the calculated value.

$\mu_{r2} = 0.0025$ is the friction factor of a needle bearing with a retainer at low speed operating without tilt of the needle roller. In fact, the crowded needle bearing without retainer used for the AT will make the needle roller tilt due to the radial and

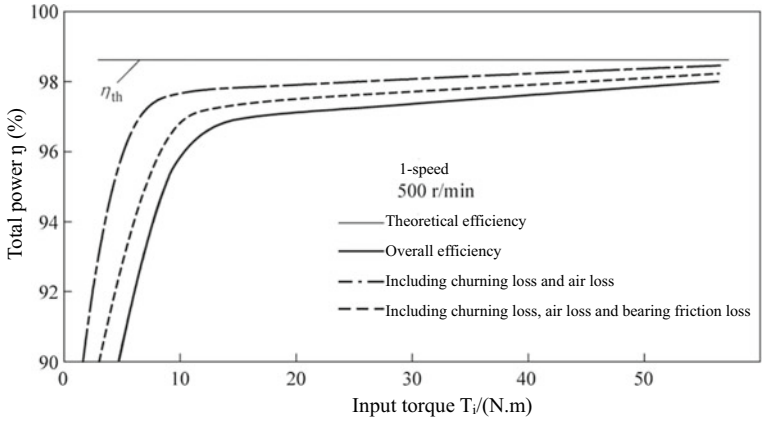

Fig. 11.29 Analysis of 1 speed gear test results

axial loads in the planetary gear train. That is, the roller rotates in the tilt condition, which will lead to an increase in the rotational resistance under unchanged load, i.e. increase in the friction factor. Moreover, when the speed reaches above a few hundred revolutions per minute, the influence of the needle roller tilt on friction factor will be more serious. Therefore, the needle bearing friction factor $\mu_R = 0.010$ inversed from the test is reliable. The analysis of the 2 speed gear test results is shown in Fig. 11.30.

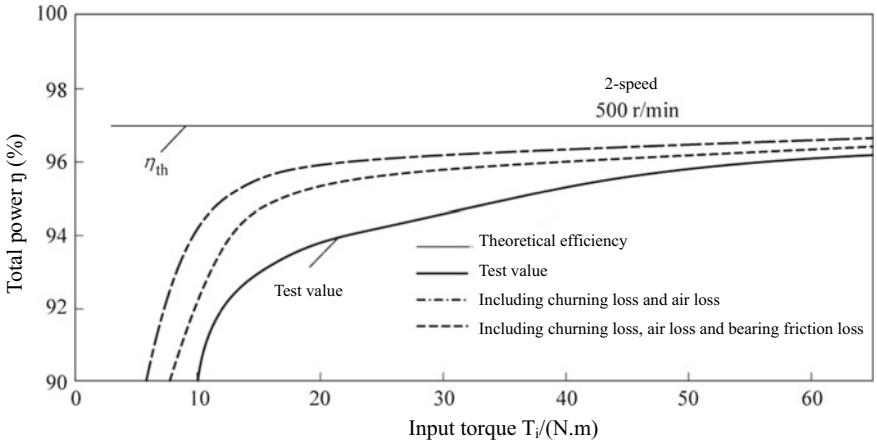

Fig. 11.30 Analysis of 2 speed gear test results

11.3 Theoretical Calculation of Vibration and Noise of Planetary Gear Train

Gear noise is the main problem of AT noise. From low speed to high speed, noise is generated in gear engagement under various operating conditions. The planetary gear train is a gear mechanism in which several planetary gears are meshed with the center gear and gear ring simultaneously and its characteristics are different from the external meshed gear.

Due to the pitch error, tooth contour error and tooth profile error in the planetary gear train, even if the input speed is constant, the output speed will fluctuate periodically, which will affect the fatigue life of the mechanism and generate noise.

The noise is generated in gear engagement when the vehicle is driving under various conditions. How to reduce noise and vibration is an important subject in transmission design.

I. Planetary gear layout

In the planetary gear train, the number of planetary gears shall satisfy a certain relation: the angle between the lines of the center of two adjacent planetary gears and the center of the planetary gear train shall be an integral multiple of $\frac{360^\circ}{z_A+z_C}$; the planetary gears shall be spaced at the same intervals and the number of planetary gears shall be an integral multiple of $\frac{360^\circ}{z_A+z_C}$, as shown in Fig. 11.31. Here, z_A is the number of teeth of center gear and z_C is the number of teeth of gear ring.

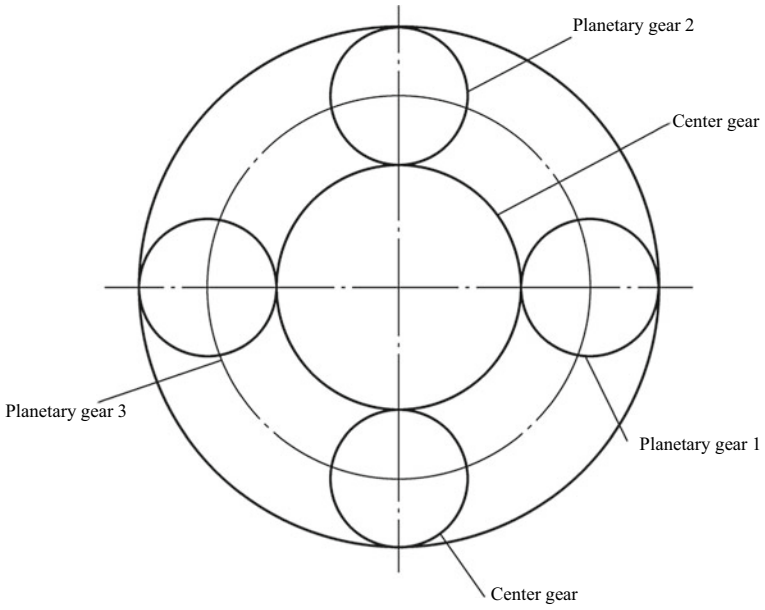

Fig. 11.31 Planetary gear layout requirements

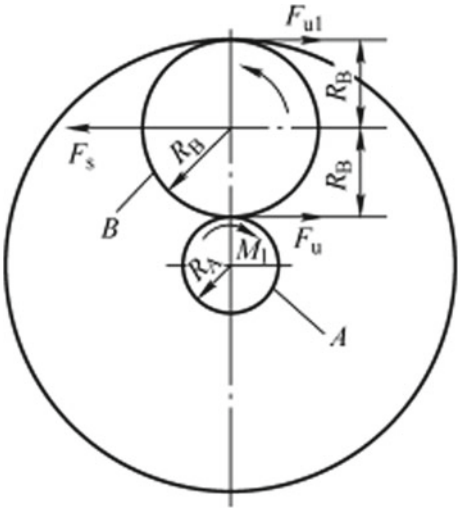

Fig. 11.32 Force on single planetary gear

The number of teeth of planetary gear z_B is determined by

$$\begin{cases} z_C - z_B = z_A + z_C \\ z_B = (z_C - z_A)/2 \end{cases} \tag{11.42}$$

II. **Planetary gear mesh cycle**

There is a certain error in the gear. Even if the uniform angular velocity is input, the output angular velocity will also fluctuate periodically, which may affect the fatigue life of the planetary gear train and cause noise problems.

As shown in Fig. 11.32, the circumferential force of the center gear acting on the planetary gear is $F_u = M_1/R_A$ and of the gear ring acting on the planetary gear is F_{u1}. According to the torque balance, F_u and F_{u1} have the same magnitude and direction; according to the force balance, the force between the planetary carrier and planetary gear is $F_s = 2F_u$.

As shown in Fig. 11.33, in the meshing process, a single planetary gear is subject to two dynamic loads from the gear ring and sun gear and these two dynamic loads often have different cycles. According to the phase relation, the resultant forces acting on different planetary gears at the same time would be different.

III. **Analysis of meshing phase difference and torsional vibration of planetary gear**

When the number of teeth of center gear and the number of teeth of gear ring can be exactly divided by the number of planetary gears, different planetary gears have the same meshing phase and have the same load at the same time. It can be seen from the force analysis in Fig. 11.33 that the resultant force of the force acting on the gear ring and center gear respectively is 0 and the resultant moment on the center gear is

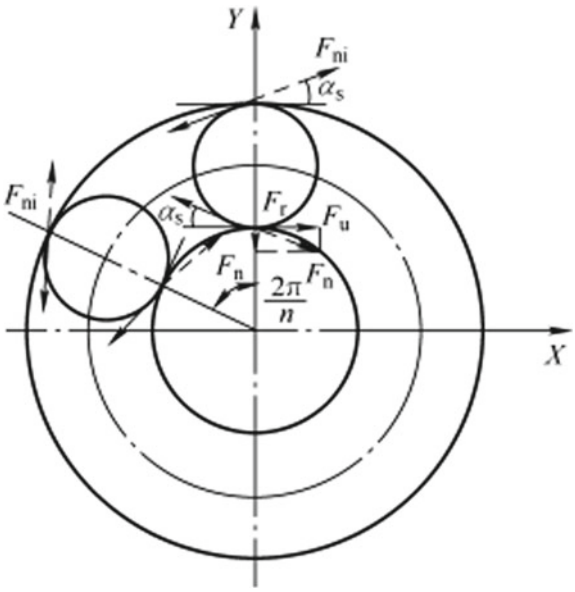

Fig. 11.33 Force on two planetary gears

$$\sum M = nR_a F_n \cos\alpha_n \tag{11.43}$$

where,

R_a—pitch radius of center gear;
F_n—normal force on tooth surface;
α_n—pressure angle.

The relationship between normal load change and torsional vibration of center gear can be obtained by the above equation.

When the number of teeth of center gear and the number of teeth of gear ring cannot be exactly divided by the number of planetary gears, planetary gears bear different load at the same time due to different meshing phases, which will affect the resonance of the gear ring, and the effect of manufacturing error will be smaller.

The meshing phase difference $\Delta\theta$ can be changed by changing the relationship among the number of teeth of center gear, the number of teeth of gear ring and the layout angle of the planetary gear. The gear ring of the planetary gear train in the AT for the passenger vehicle is of thin-walled structure and the deformation under the load may make the gear ring meshed evenly with the planetary gears, so the vibromotive force of the planetary gear train is mainly affected by the meshing of the center gear and planetary gear.

To make the phase difference exist, the number of teeth shall meet the conditions under the premise of evenly distributed planetary gears

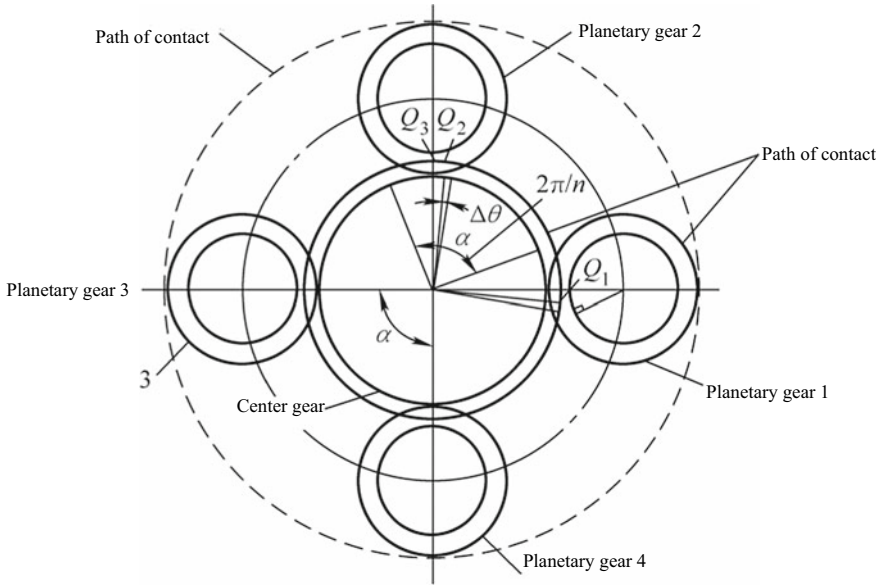

Fig. 11.34 Meshing phase difference between center gear and planetary gear

$$\begin{cases} (z_A + z_C)/n = \text{integer} \\ z_A/n \neq \text{integer} \end{cases} \tag{11.44}$$

Figure 11.34 is the schematic diagram of the meshing phase difference between the center gear and planetary gear. It is assumed that the point Q_2 is located on the planetary gear 2 and has no phase difference with the starting meshing point (point Q_1) at the dedendum of planetary gear 1 and the addendum of center gear. If the actual meshing point Q_3 of the planetary gear 2 is made rotate to Q_2 around the gear train center, the angle $\Delta\theta$ of rotation is the meshing phase difference.

The noise of the planetary gear train is mainly from the torsional vibration in the system. If the meshing phase of all planetary gears is different, the periodic vibration of planetary gear meshing with the center gear and gear ring will be significantly reduced.

The phase difference between the jth planetary gear and the center gear at the beginning of meshing of a tooth is

$$\Delta\theta = kj \times 2\pi Z'/n \tag{11.45}$$

where,

Z'—remainder of division of the number of teeth of sun gear by the number of planetary gears;
j—planetary gear code;
k—harmonic order.

When the harmonic order is k, the vibromotive force F_{kj} of the meshing between the jth planetary gear and the center gear is

$$F_{kj} = F_{nkj} \sin\left(k\omega t + kj \times 2\pi Z'/n\right) \tag{11.46}$$

where,

F_{nkj}—amplitude of the force acting on the gear (maximum value).

The relationship between the total torque of the force on the planetary gears and the pitch conforms to the sine law. If the amplitude of the loads is equal, the total torque is

$$\begin{aligned} M_k &= \sum_{j=1}^{n} F_{nk} R_B \cos\alpha_n \\ &= F_{nk} R_B \cos\alpha_n \sum_{j=1}^{n} \sin\left(k\omega t + kj \times 2\pi Z'/n\right) \end{aligned} \tag{11.47}$$

where,

R_B—pitch radius of planetary gear;
α_n—pressure angle.

If M_k is 0 and the calculated value of the meshing transfer error caused by the rigidness is 0, the torsional vibration will not appear.

Figure 11.35 shows 1 speed planetary gear train with phase difference. Because of the phase difference, the sinusoidal forces generated in meshing cancel each other, and the vibromotive force of meshing is 0.

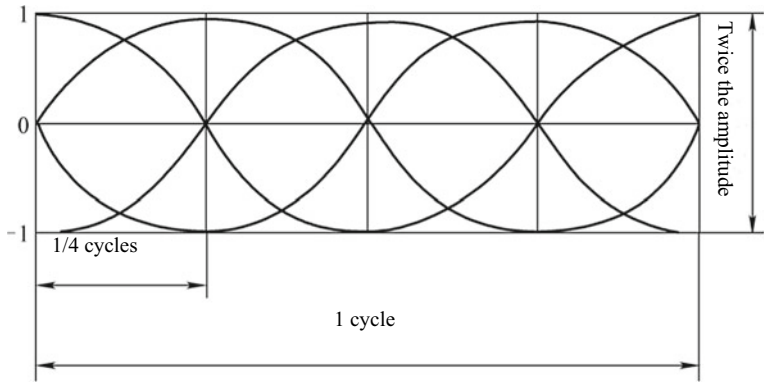

Fig. 11.35 1 speed planetary gear train with phase difference

IV. **Calculation of phase difference of test planetary gear train**

The 1 speed planetary gears are evenly distributed and have proper meshing phase difference, so that the vibromotive force at the meshing positions cancels each other. In case of no manufacturing error in the gear, the vibromotive force of meshing is 0 theoretically.

The meshing phase difference of the planetary gear train is

$$\Delta\theta = \frac{2\pi}{z_A} H - \frac{2\pi}{n} \tag{11.48}$$

where,

H—an integer;
n—number of planetary gears;
z_A—number of teeth of center gear, with the formula as

$$z_A = nH \pm 1 \tag{11.49}$$

It is calculated from formula (11.48) that the meshing phase difference of the 1 speed gear is $\Delta\theta = 2.432°$.

The meshing frequency is one of the reasons that affect the gear noise and vibration. Through spectral analysis of the gear noise and vibration frequency, the peak occurs at the doubling of the meshing frequency. The noise and vibration are also affected by gear dynamic load.

The meshing frequency f_z of the 1 speed planetary gear is the number of meshing teeth of the planetary carrier (output) per revolution. The number of meshing teeth can be calculated from the relative speed between the center gear and the planetary carrier

$$(n_A - n_S)z'_A = \left(n_A - \frac{n_A z'_A}{z'_A + z'_C}\right) z'_A = \frac{n_A z'_C z'_A}{z'_A + z'_C} \tag{11.50}$$

where,

z'_A—number of teeth of sun gear in second planetary gear set;
z'_C—number of teeth of gear ring in second planetary gear set;
n_A—sun gear speed (r/min);
n_S—planetary carrier speed (r/min).

Input shaft speed in gear 1 (r/min) $n_i = n_A$ and meshing frequency

$$f_z = \frac{n_i z'_C z'_A}{60\left(z'_A + z'_C\right)} \tag{11.51}$$

Through calculation

$$f_z = 0.413 n_i$$

The number of meshing teeth of the 4 speed planetary gear is calculated from the relative speed between the gear ring and the planetary carrier

$$(n_C - n_S) z_C = \left(\frac{n_S (z_A + z_C)}{z_C} - n_S \right) z_C = n_S z_A \tag{11.52}$$

where,

z_A—number of teeth of center gear in second planetary gear set;
z_C—number of teeth of gear ring in second planetary gear set;
n_S—planetary carrier speed (r/min);
n_C—gear ring speed (r/min).

Input shaft speed in gear 4 (r/min) $n_i = n_S$ and meshing frequency

$$f_z = \frac{n_i z_A}{60} \tag{11.53}$$

Through calculation

$$f_z = 0.55 n_i$$

Because there are several pairs of gears meshed in a gear assembly, there will be more than one vibration frequency. To analyze the vibration frequency, it is necessary to calculate the meshing times of each gear pair.

Meshing times of each gear pair in gear 1: gear ring $1.321 n_i$; center gear $2.678 n_i$; planetary gear $1.304 n_i$.

Meshing times of each gear pair in gear 4: center gear $3 n_i$; gear ring $1.32 n_i$; planetary gear $1.571 n_i$.

11.4 Vibration and Noise Test of Planetary Gear Train

A power absorption type gear test bench is used to test the planetary gear trains with phase difference (1 speed) and without phase difference (4 speed) respectively. The vibration and noise of the planetary gear train can be measured by changing the meshing rate, accuracy, load and speed.

The power absorption type gear test bench is shown in Fig. 11.36. In order to accurately measure the noise generated by the planetary gear train, the motor, the reducer and the planetary gear train in the dashed box are placed in the sound insulation box for sound insulation, so as to reduce the dark noise to less than 6 dB.

The lubricant is ATF, which is supplied to the planetary gear train from three injectors near the center gear and one injector in the upper part of the center gear,

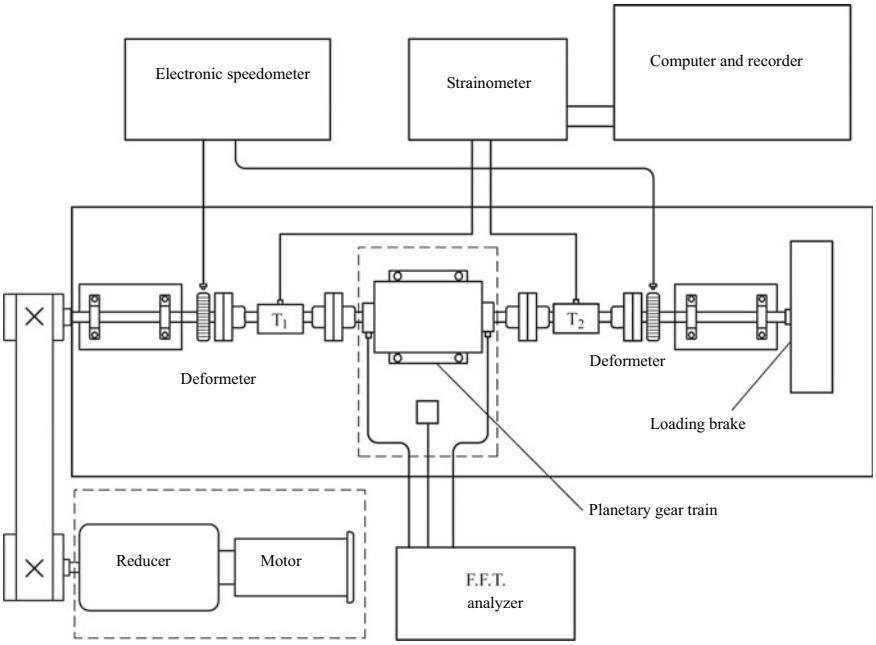

Fig. 11.36 Power absorption type gear test bench

at the flow rate of 1.5 L/min and the temperature of (32 ± 2) °C. The input torque range is 0–80 N m, and the speed of high speed shaft (input shaft) is 500–2400 r/min. The speed changes 100 r/min each time, and the torque changes 5 N m each time. An acceleration vibration sensor is installed near the supports of the input shaft and the output shaft to measure the vibration acceleration and noise of the planetary gear train.

I. **Small load test for shaved gears**

Figures 11.37 and 11.38 show the results of the small load test for shaved gears. The test gear parameters are the high-tooth gear pair A in Table 11.1. "□" means 1 speed gear (with phase difference) and "△" means 4 speed gear (without phase difference). The input speed is 500–2400 r/min, the input torque in gear 1 is 20 N m, and in gear 4 is 43 N m.

As can be seen from the figure, the noise level of the planetary gear train with phase difference is 3–8 dB lower than that without phase difference, and the vibration level is 2–4 dB lower. The test results show that the existence of phase difference can significantly reduce the torsional vibration, and the design of phase difference is an effective way to reduce the vibration and noise of the planetary gear train.

II. **Large load test for shaved gears**

Figures 11.39 and 11.40 show the results of the large load test for shaved gears. The input torque in gear 1 is 40 N m, and in gear 4 is 80 N m. It can be seen from the

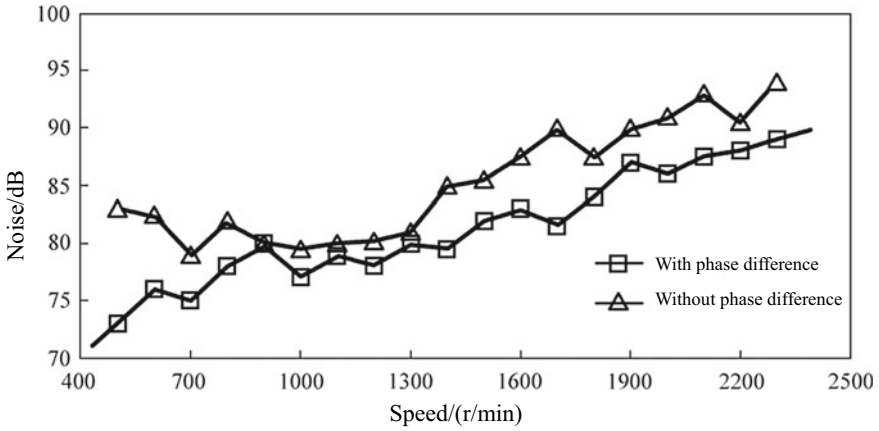

Fig. 11.37 Influence of shaved gear (small load) phase difference on noise

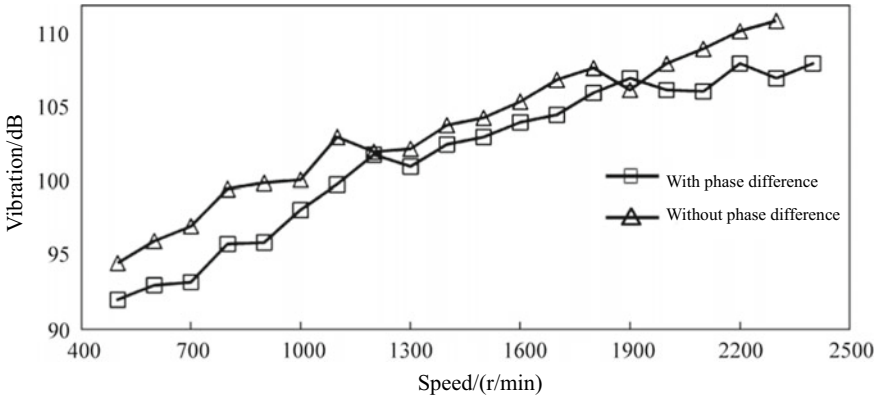

Fig. 11.38 Influence of shaved gear (small load) phase difference on vibration

figure that under the same operating conditions, compared with the gear grinding process, the change law of the two curves is almost the same. It can be considered that the elastic deformation of gear teeth is the main cause for vibration and noise under large load conditions.

III. **Small load test for ground gears**

The planetary gear and center gear for test are ground by the MAAG gear grinding machine to the accuracy up to JIS 0–1. The test results are shown in Figs. 11.41 and 11.42. As can be seen from the figure, the noise level of the planetary gear train with phase difference is 6–10 dB lower than that without phase difference within the test speed range and the accuracy of ground gear has relatively small influence on the test results; in the case of phase difference and no phase difference, the vibration level is

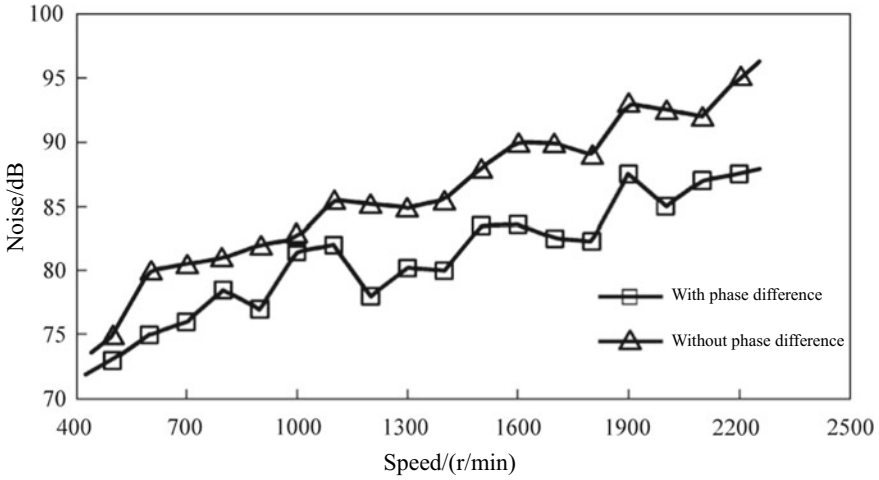

Fig. 11.39 Influence of shaved gear (large load) phase difference on noise

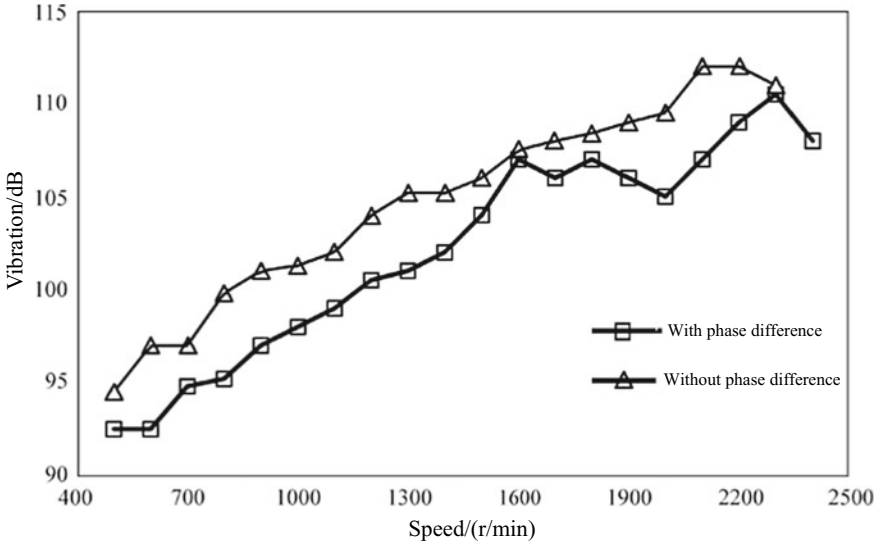

Fig. 11.40 Influence of shaved gear (large load) phase difference on vibration

basically the same with the increase of the speed. The vibration level of gear with 1 gear (with phase difference) is 2–4 dB lower than that with 4 gears (without phase difference).

Tables 11.4 and 11.5 list the vibration and noise level data of the 1 speed (with phase difference) and 4 speed (without phase difference) in the frequency range of 0–10 kHz and 0–5 kHz respectively.

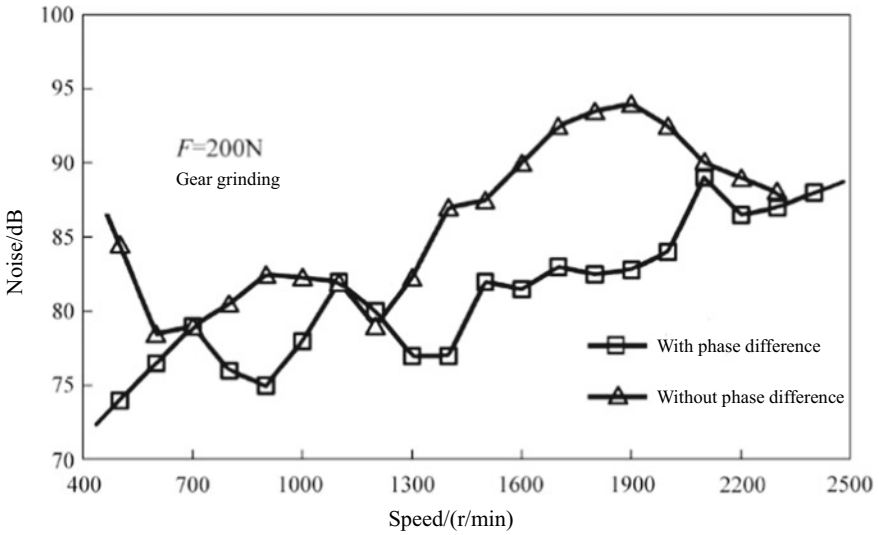

Fig. 11.41 Influence of ground gear (small load) phase difference on noise

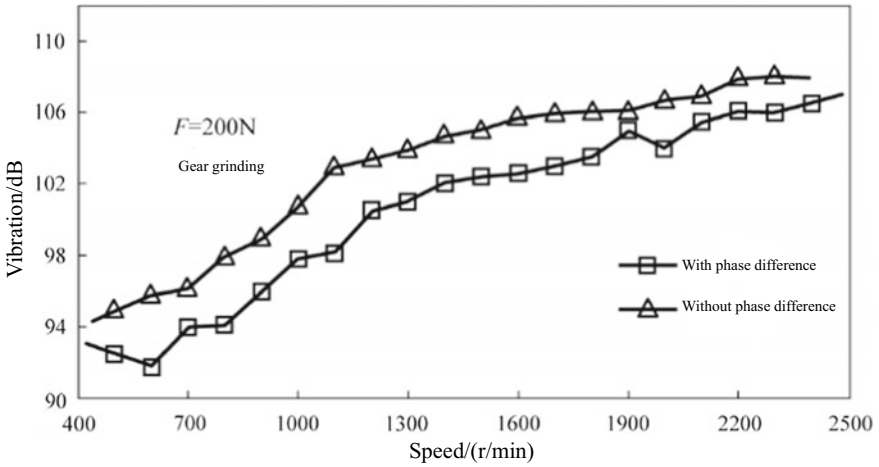

Fig. 11.42 Influence of ground gear (small load) phase difference on vibration

IV. **Large load test for ground gears**

It is set in the test that the input speed is 500–2400 r/min, the input torque in gear 1 is 40 N m, and in gear 4 is 80 N m (tangential load 370 N). The noise level curve from the test is shown in Fig. 11.43. As can be seen from the figure, the noise level of the planetary gear train with phase difference is 3–9 dB lower than that without phase difference. Compared with the test results when the tangential load of the tooth

Table 11.4 Noise level data

Speed/(r/min)	Noise/dB (0–10 kHz)		Speed/(r/min)	Noise/dB (0–5 kHz)	
	1 speed gear	4 speed gear		1 speed gear	4 speed gear
500	74.21	84.68	500	71.30	83.28
600	74.21	78.76	600	76.48	83.68
700	79.19	79.21	700	78.27	82.72
800	72.17	81.00	800	75.66	82.76
900	75.19	82.73	900	81.27	83.15
1000	78.03	82.50	1000	77.69	77.94
1100	82.22	82.00	1100	78.30	79.52
1200	79.97	78.83	1200	76.68	80.82
1300	76.95	82.68	1300	80.66	82.34
1400	76.93	87.45	1400	81.35	86.02
1500	81.58	87.59	1500	82.80	86.79
1600	81.28	90.55	1600	83.95	91.70
1700	83.72	82.92	1700	84.63	91.57
1800	82.53	93.71	1800	81.88	93.71
1900	83.51	94.00	1900	86.19	95.52
2000	84.26	92.55	2000	88.11	92.64
2100	89.06	90.29	2100	86.26	91.96
2200	86.40	89.14	2200	87.44	87.98
2300	87.09	87.98	2300	90.04	90.66
2400	88.37		2400	89.18	

surface is 200 N, the influence of phase difference on the noise level is more obvious after the increase of input torque.

Figure 11.44 shows the influence of phase difference on vibration. As can be seen from the figure, within the range of speed change, the amplitude of vibration level change measured in the two tests is basically the same, with a difference of 3–5 dB. However, the corresponding speed of the peak value at vibration level is different from that in Fig. 11.43.

V. Influence of torque on vibration and noise of planetary gear train with phase difference

The influence of the torque on the vibration and noise of the planetary gear train at the speed 1200 r/min is shown in Figs. 11.45 and 11.46 respectively. It can be seen from the figure that the torque has little influence on noise. When the load torque is increased, the difference of vibration level tends to increase.

Table 11.5 Vibration level data

Speed/(r/min)	Noise/dB (0–10 kHz)		Speed/(r/min)	Noise/dB (0–10 kHz)	
	1 speed gear	4 speed gear		1 speed gear	4 speed gear
500	92.27	94.69	500	90.90	93.49
600	91.62	95.41	600	92.79	94.78
700	93.87	96.45	700	93.57	95.38
800	94.27	98.30	800	94.29	96.91
900	95.68	99.53	900	95.83	97.94
1000	97.47	101.00	1000	96.67	98.71
1100	98.53	102.96	1100	97.11	103.91
1200	100.37	103.05	1200	97.64	101.90
1300	100.94	104.10	1300	99.22	101.91
1400	102.10	104.68	1400	99.93	102.15
1500	102.46	105.37	1500	99.92	103.44
1600	102.82	105.68	1600	100.19	103.22
1700	102.98	106.07	1700	101.20	102.58
1800	103.12	106.10	1800	101.70	103.29
1900	105.44	106.32	1900	103.74	103.90
2000	104.33	107.10	2000	104.94	105.52
2100	105.84	107.74	2100	104.90	105.45
2200	106.76	108.56	2200	103.60	108.21
2300	106.17	108.77	2300	103.39	106.97
2400	107.09		2400	107.96	

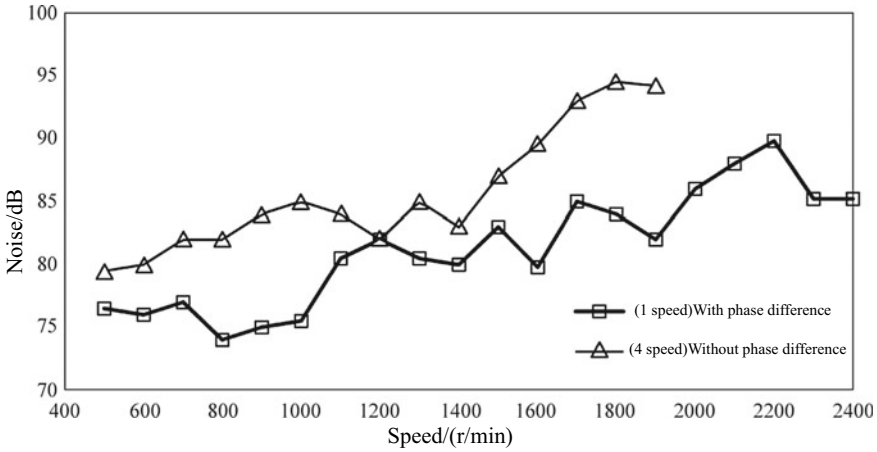

Fig. 11.43 Influence of ground gear (large load) phase difference on noise

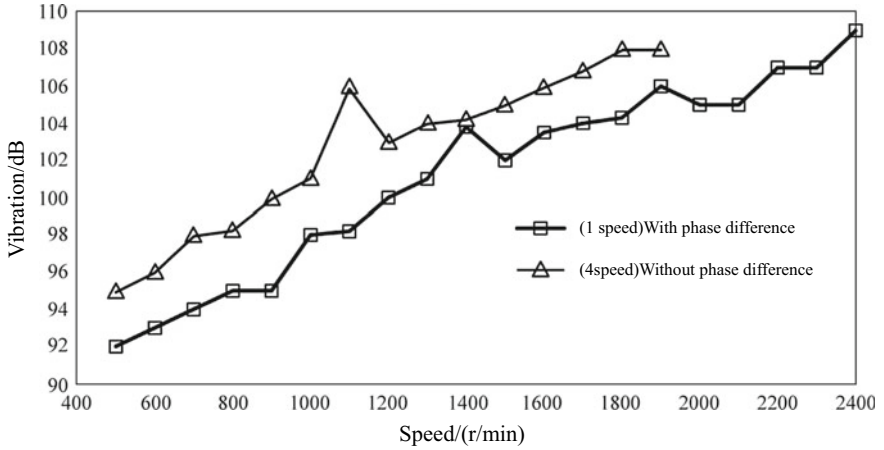

Fig. 11.44 Influence of ground gear (large load) phase difference on vibration

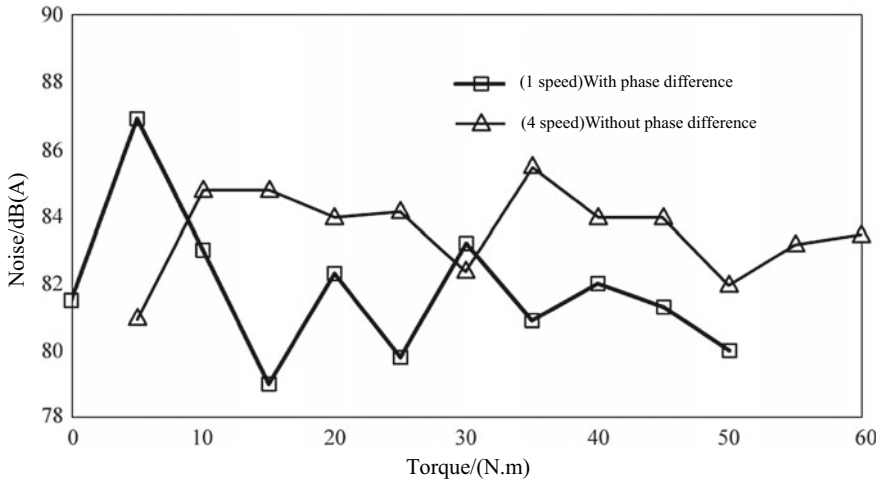

Fig. 11.45 Influence of torque on noise

VI. Influence of contact ratio on vibration and noise of planetary gear train with phase difference

See Table 11.1 for the parameters of 1 speed in the test. High-tooth gear pair A (1.65/1.81) and standard gear pair B (1.30/1.66) are selected, and the input shaft speed is 500–2400 r/min. It can be seen from Figs. 11.47 and 11.48 that two gear pairs are tested respectively with 200 N tangential load on tooth surface, and there is no significant difference in noise and vibration levels. The reason is that the contact ratio of the 1 speed planetary gear train is large, and the gear offsets the vibromotive force caused by the stiffness and flexibility.

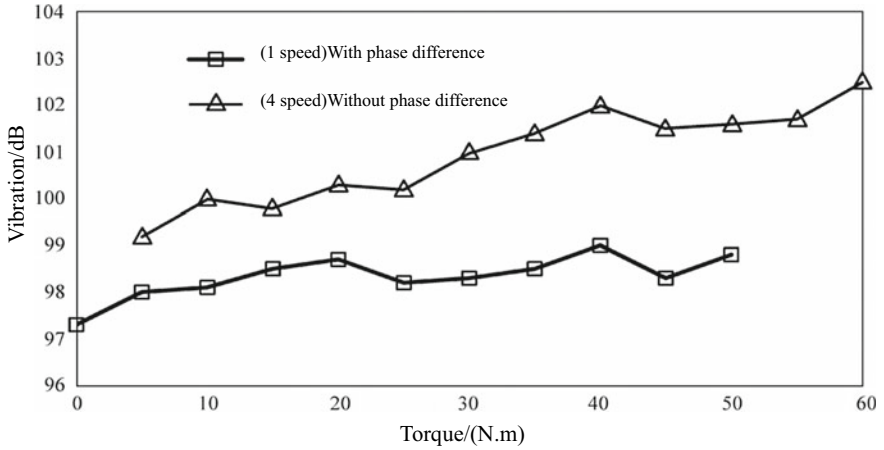

Fig. 11.47 Influence of contact ratio on vibration

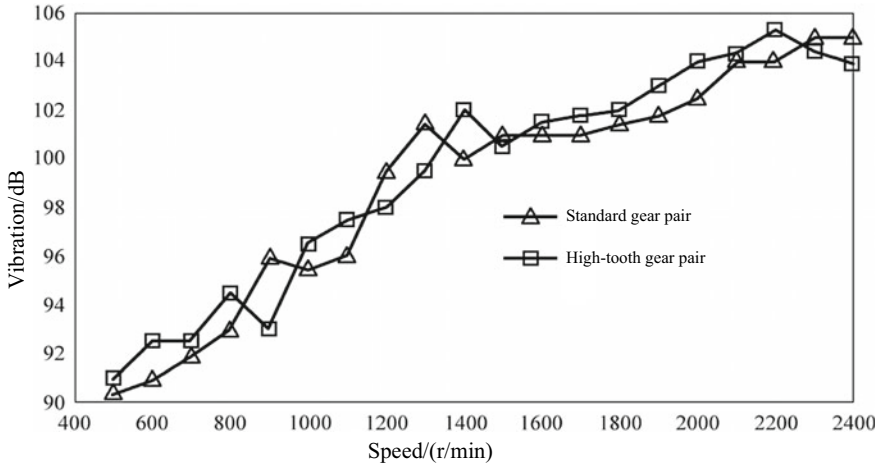

Fig. 11.46 Influence of torque on vibration

VII. **Influence of accuracy on vibration and noise of planetary gear train with phase difference**

In the two gear pairs used in the test, one dual-planetary gear set of planetary gear and center gear is subject to gear shaving, carburizing and quenching and the other set is ground by MAAG gear grinding machine after gear shaving, carburizing and quenching. The accuracy of the former is JIS 3–4 and the tooth surface roughness is about R_{amax} 6 μm (R_a 1.5 μm); the accuracy of the latter is JIS 0–1 and the tooth surface roughness is R_{amax} 2 μm (R_a 0.5 μm). The test results are shown in Fig. 11.49 and 11.50. As can be seen from the figures, the vibration and noise level of the ground

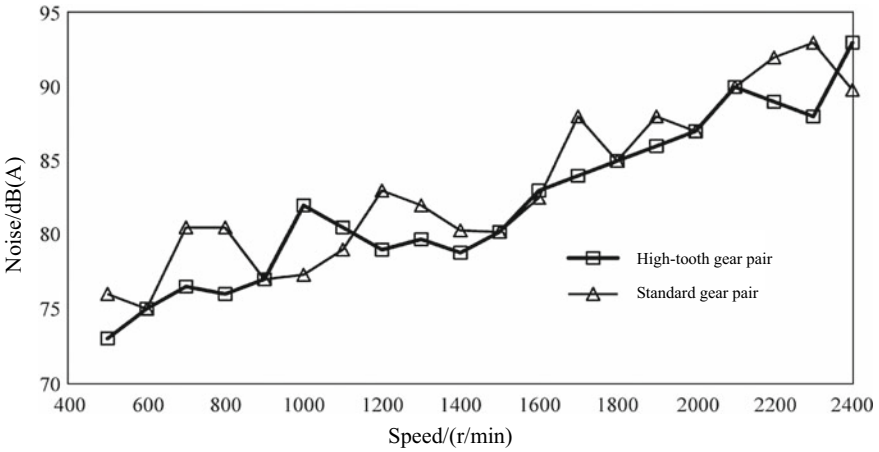

Fig. 11.48 Influence of contact ratio on noise

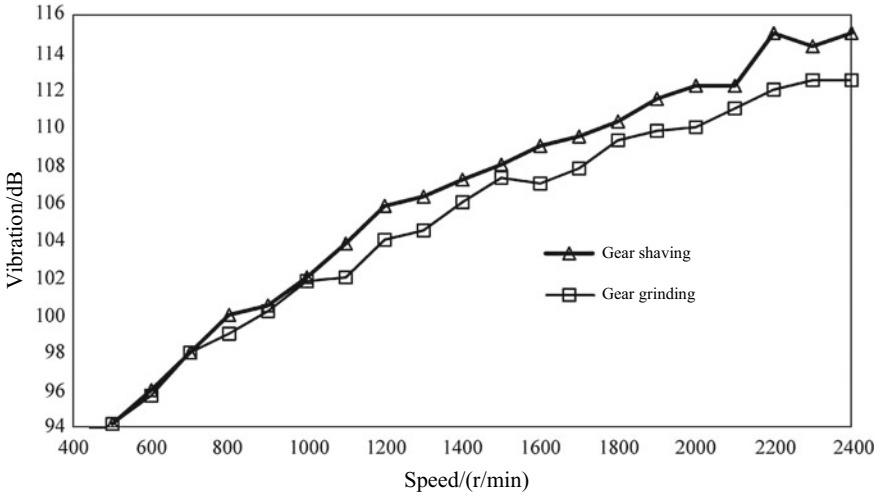

Fig. 11.49 Influence of accuracy on vibration

high-accuracy gear is 2–3 dB lower than that of the gear without grinding. Especially when the speed reaches above 1000 r/min, the difference of vibration level is more obvious.

VIII. **Influence of torque on vibration and noise of planetary gear train of different accuracy with phase difference**

The gear used in the test is 1 speed planetary gear train with phase difference, and there are two kinds of processing technology, namely gear shaving and grinding. As shown in Figs. 11.51 and 11.52, the input shaft speed is 1200r/min, and the input

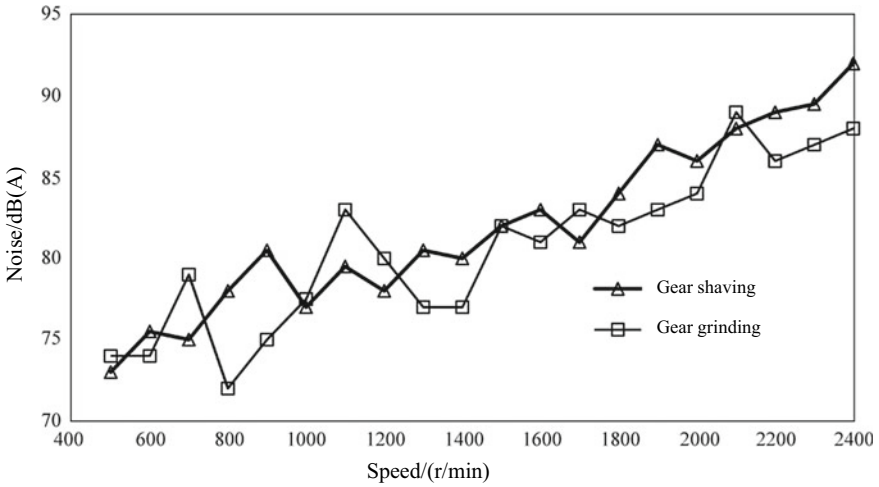

Fig. 11.50 Influence of accuracy on noise

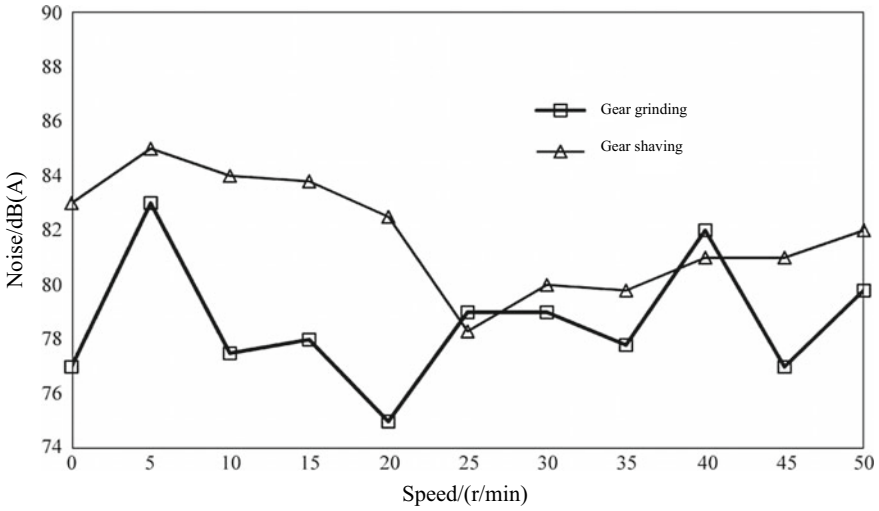

Fig. 11.51 Influence of torque on the noise of planetary gear train of different accuracy

torque change range is 0–50 N m. As can be seen from the figures, when the input torque exceeds 10 N m, the vibration and noise levels tend to increase with the increase of torque. In the test torque range, the vibration noise of the ground gear is lower.

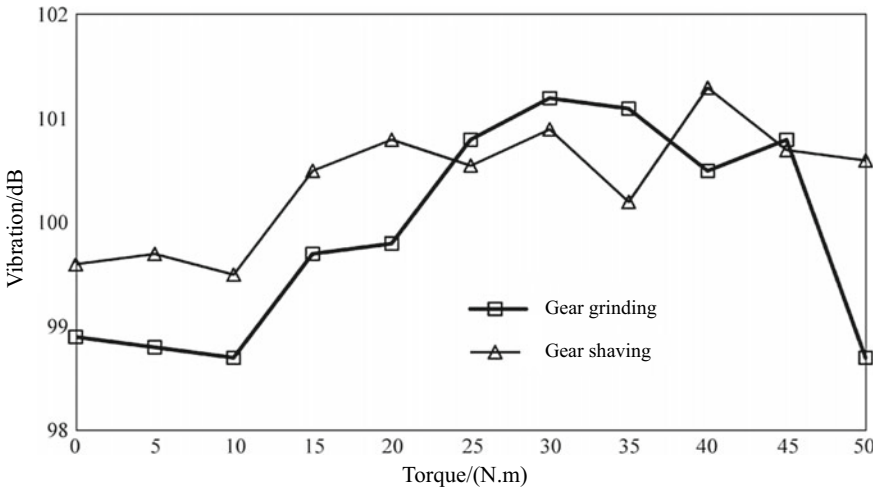

Fig. 11.52 Influence of torque on the vibration of planetary gear train of different accuracy

IX. **Analysis of vibration and noise test results**

Figures 11.53 and 11.54 show the spectral analysis results of the vibration and noise of the 1 speed planetary gear with phase difference. Test conditions: gear grinding, tangential load 200 N and input shaft (high speed shaft) speed 1600 r/min.

The meshing frequency of the planetary gear is 660 Hz, and the peak of vibration and noise acceleration level corresponding to the frequency doubling could not be clearly identified. The reason is that there is phase difference in the meshing of planetary gear and center gear, and the vibration caused by phase difference is exactly offset with the torsional vibration caused by the planetary gear.

Figures 11.55 and 11.56 show the spectral analysis results of the vibration and noise of the 4 speed planetary gear without phase difference and the test conditions are the same as those for spectral analysis of 1 speed. Compared with that with phase

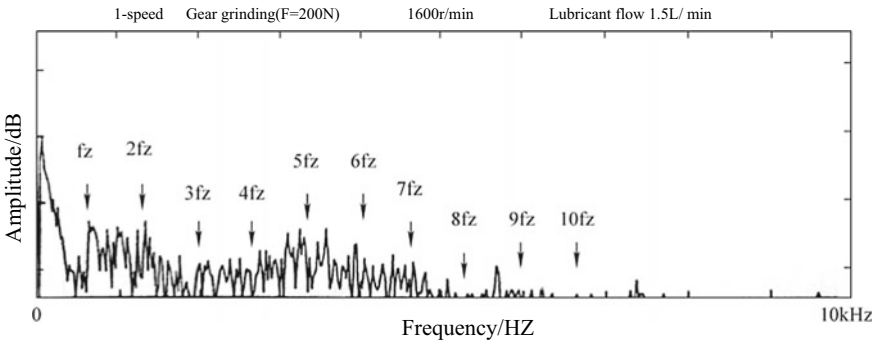

Fig. 11.53 Spectral analysis results of vibration of 1 speed planetary gear

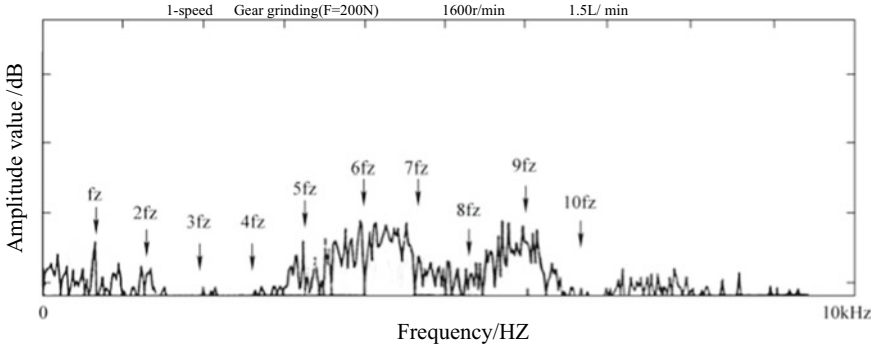

Fig. 11.54 Spectral analysis results of noise of 1 speed planetary gear

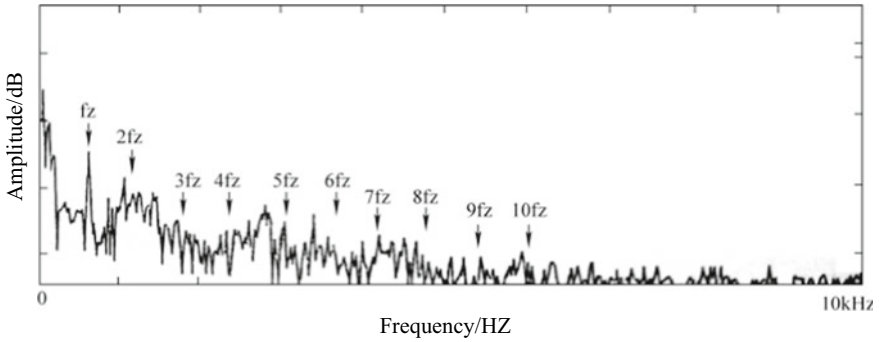

Fig. 11.55 Spectral analysis results of vibration of 4 speed planetary gear

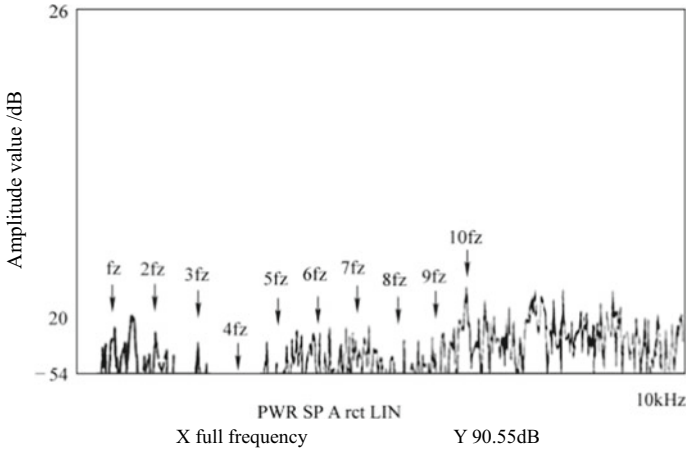

Fig. 11.56 Spectral analysis results of noise of 4 speed planetary gear

difference, the noise level without phase difference is about 9 dB higher, and the vibration acceleration level is about 3 dB higher. The meshing frequency of planetary gear is 611 Hz, and the corresponding vibration and noise levels are much higher when the harmonic order is 1–3 times than that with phase difference. It can be seen from the figure that the circumferential vibration acceleration of the planetary gear train is formed by the superposition of vibration of the integer multiple frequencies in the meshing frequency. The total stiffness of the planetary gears without phase difference is a multiple of the number of planetary gears and the vibromotive force will increase in the periodically varying meshing.

Bibliography

1. Mitschke M, Wallentowitz H (2009) Automobile dynamics (Translated by Yinsan C, Qiang Y). Tsinghua University Press, Beijing
2. Hongxin Z (1996) Auto design. Version 2. China Machine Press, Beijing
3. Wangyu W (2017) Auto design. Version 2. China Machine Press, Beijing
4. Li C (2005) Study on efficiency of planetary gear train of automatic transmission. Chongqing University, Chongqing